EXPERIMENTAL INVESTIGATION OF SHEAR CAPACITY OF PRECAST REINFORCED CONCRETE BOX CULVERTS

by

JARROD CLINTON BURNS

Presented to the Faculty of the Graduate School of

The University of Texas at Arlington in Partial Fulfillment

of the Requirements

for the Degree of

MASTER OF SCIENCE IN CIVIL ENGINEERING

THE UNIVERSITY OF TEXAS AT ARLINGTON

December 2006

ACKNOWLEDGEMENTS

This document is dedicated to the love and devotion of my wife, Dior, and my family in Arkansas. Their support during these past two years has been invaluable, and they have continued to motivate me to do my very best. The Lord Jesus Christ is to receive all the glory for this research and for my salvation.

I would like to thank the National Highway Institute for the Eisenhower Transportation Fellowship that funded my education. I would also like to thank Dr. Ali Abolmaali for investing his time in me and believing in my potential. Additionally, a special thanks goes to Dr. Raul Fernandez for his expertise and friendship during this project. Deep gratitude is also paid to Anil Garg for his hard work and friendship.

Others I would like to thank include the National Science Foundation's Research Experience for Undergraduates program. The hard work of Winston, Richard, Francesca and Jeremy made this research possible. The American Concrete Pipe Association for funding the research materials and related project costs. Special thanks to Paul Shover for setting up each load test. I would also like to thank the many friends that I made during my two years at the University of Texas at Arlington. The friendships I built there made the hard work worth every minute.

November 10, 2006

ABSTRACT

EXPERIMENTAL INVESTIGATION OF SHEAR

CAPACITY OF PRECAST REINFORCED

CONCRETE BOX CULVERTS

Publication No. _____

Jarrod Clinton Burns, M.S.

The University of Texas at Arlington, 2006

Supervising Professor: Ali Abolmaali

This study presents the experimental investigation of the shear capacity of four precast reinforced concrete box culverts. Each culvert was subjected to a monotonically increasing load through a 20-in x 10-in load plate, designed to simulate a standard HS 20-44 wheel footprint. Each box was instrumented with the following: strain gages, load cell, high-resolution laser sensor, data acquisition hardware and software, and laptop computer. The tests were conducted on 1.22 m x 1.22 m x 1.22 m (4 ft x 4 ft x 4 ft) box culverts, with load being applied at the free spigot end. The location of the load

plate in relation to the span varied for each test in order to induce maximum shear stresses. Results of physical load tests indicate that free culvert ends are adequate in shear without the use of edge beams. The results from each test detailed herein are intended to provide data for the verification and convergence of an analytical model currently under development.

TABLE OF CONTENTS

LIST OF ILLUSTRATIONS

LIST OF TABLES

CHAPTER I

INTRODUCTION

1.1 Introduction

Since 1994, the American Association of State Highway and Transportation Officials (AASHTO) has slowly begun to implement a new set of specifications for highway bridge design based on Load Resistance Factor Design. Now in its third edition (LRFD 2004), the LRFD Bridge Design Specifications are quickly approaching mandatory implementation across the United States while the preceding Standard Specifications are being retired (AASHTO 2002). Many of the design concepts and procedures included in the LRFD Specifications have already been evaluated and accepted. However, this is not the case for shear capacity of reinforced concrete box culverts with less than 0.61 m (2 ft) of fill. The governing equations for such culverts published in the early editions of the LRFD Specifications have been under scrutiny because they were derived from the research of reinforced concrete bridge decks spanning parallel to traffic. Some argued that this type of deck does not directly correlate to box culvert spans because of the difference in stiffness.

Recent interim specifications (LRFD 2005) present revised criteria for both the analysis and design of box culverts based on analytical research (McGrath et al. 2004). Particularly, the live load distribution widths have been adjusted (LRFD 2005, 4.6.2.10) and a new requirement for edge beams has been presented (LRFD 2005, 12.11.2.1).

The research by McGrath et al. was purely analytical and only examined one case in which the span length was shorter than 4.57 m (15 ft), the length at which the governing LRFD equations change. In order to investigate the accuracy of the analytical results and recommendations made by McGrath et al., the research presented in this report was performed.

The research detailed herein presents physical load test results of four 1.22 m x 1.22 m x 1.22 m (4 ft x 4 ft x 4 ft) precast concrete box culverts. Each culvert was tested at the free spigot end in order to investigate the need for the aforementioned edge beam criteria. This report details load testing setup and procedures, instrumentation and data acquisition systems, load test results, research conclusions, and recommendations.

1.2 Background

The use of concrete channels for the purpose of supplying drinking water and disposing of sewage dates back to the aqueducts of ancient Rome. Concrete has proven to be a long lasting material as portions of the aqueducts are still utilized today. As civilizations concentrated into villages, towns, and eventually cities, transferring large amounts of storm water became a concern. Land-uses changed; areas that were previously open fields and forests became covered by pavement and buildings that shed water quickly and caused flash floods. As a result, a need for transferring storm water from civilized areas became an integral part of urban infrastructure systems. Over the centuries, the concepts behind the great aqueducts of Rome have evolved into various forms of infrastructure systems, each unique to its intended use.

Today, drainage systems are an essential part of life that most take for granted. Culverts of all shapes, sizes, and materials are installed in new developments everyday and continue to provide protection from flood waters while maintaining natural flows through our streams and rivers. Most drainage systems utilize concrete as the construction material of choice because of its inherent strength. As design and production techniques have evolved, concrete culverts that were once cast-in-place on the job site are now precast in fabrication plants and transported to job sites for installation.

Precast reinforced concrete box culverts (PRCB) are most often used when large amounts of storm water need to be transferred out of a developed area. The shape of a box culvert is designed to support loads above and around it while allowing storm water to pass through it. When a drainage system crosses a roadway, as they often do in low-lying areas, a PRCB can also serve as a highway bridge. Since drainage systems that utilize PRCBs are gravity fed, it is not always feasible to burry culverts below the effects of vehicle loads. Therefore, they must be utilized as both a drainage culvert and a bridge. Culverts of this type are designed using AASHTO bridge design specifications (AASHTO 2002, LRFD 2004, 2005, and 2006).

Box culverts are identified by their rise, span, and joint length dimensions [i.e. 1.22 m x 1.22 m x 1.22 m (4 ft x 4 ft x 4 ft) respectively]. The main components of a precast box culvert are the top slab, bottom slab, side walls, steel reinforcement mesh, bell end, spigot end, and haunches as shown in Figure 1.1 and Figure 1.2. The area of reinforcing steel, thicknesses of concrete, and the size of the haunches differ based on

culvert size, anticipated loading, depth of cover, and manufacturer. Precast culverts vary in span length from 0.91 m to 3.66 m (3 ft to 12 ft) and rise from 0.61 m to 3.66 m (2 ft to 12 ft). The joint length or "laying" length varies by manufacturer and is generally constructed based on the equipment available for transporting and installing the culvert. Generally, the joint length ranges between 1.22 m and 2.44 m (4 ft and 8 ft). For common designs, the thickness of concrete for the top slab ranges from 102 mm to 305 mm (4 in to 12 in) depending on the span length. The culverts are reinforced with smooth or deformed welded wire reinforcement mesh as per ASTM standards A 185 (2001) and A 497 (2001). The concrete cover on both the inside (C_i) and outside (C_o) of the culvert is specified to be the greater of three times the diameter of the welded wire reinforcement or 25 mm (1 in) (LRFD 12.11.4.4). When the height of fill is equal to or less than 0.61 m (2 ft) C_o is specified to be 51 mm (2 in) for the top slab only (LRFD 12.11.4.4). Prior to 2003, culverts were designed based on ASTM C 789 for depth of fill greater than two-feet and ASTM C 850 for depth of fill equal to or less than two-feet; however, they have now been encompassed into a single specification, ASTM C 1433 (2003). Precast boxes are typically designed to yield a concrete compressive strength of 34.5 N/mm^2 (5,000 psi). They can be produced by either drycast or wetcast methods. Drycast represents a concrete mix that utilizes a low water/cement ratio (0.35 or less) while wetcast is characterized by a high slump from 102 mm to 152 mm (4 in to 6 in) and a water/cement ratio necessary to achieve a high slump. Boxes are joined by placing the spigot end into the bell end and grouting the

joint. This is done during installation as the boxes are positioned in their desired location.

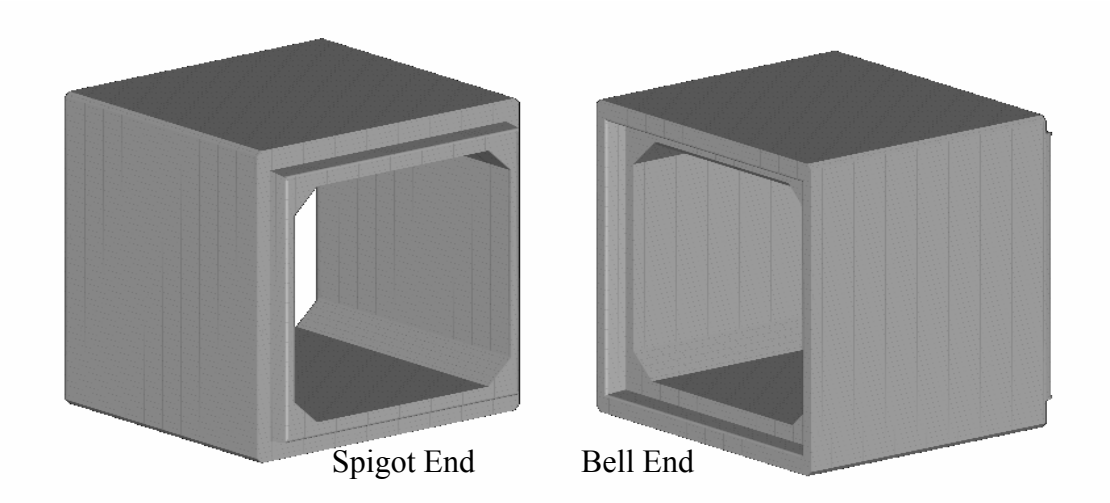

Figure 1.1: Precast Concrete Box Culvert End Designation

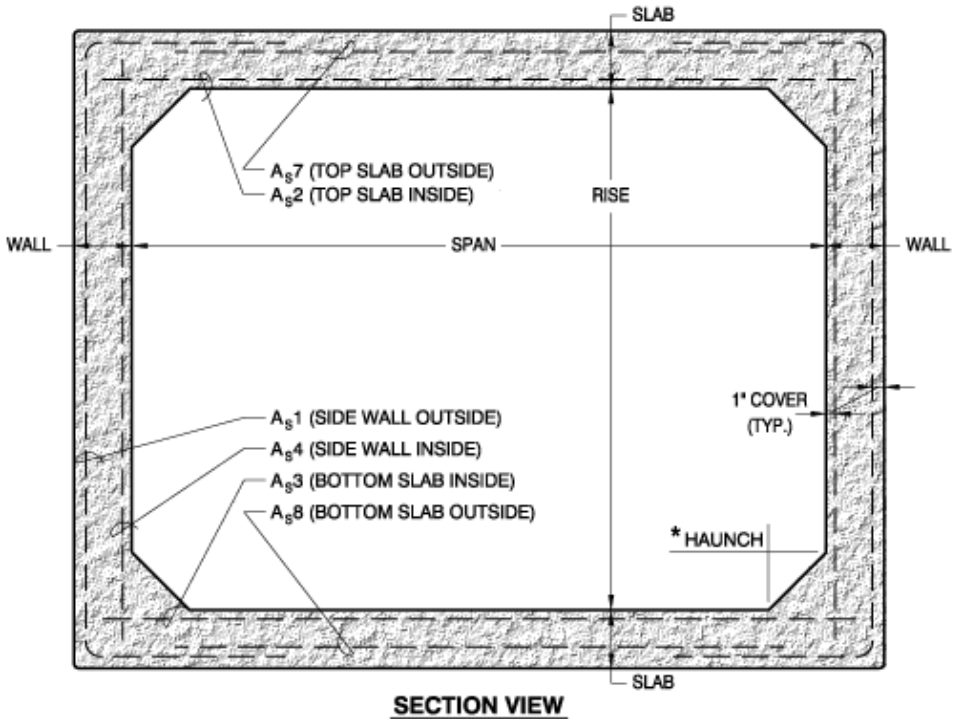

Figure 1.2: Precast Box Culvert Components

Load tests presented herein were performed on four 1.22 m x 1.22 m x 1.22 m (4 ft x 4 ft x 4 ft) precast box culverts designed for depth of fill less than 0.61 m (2 ft). The reinforcement embedded in each cage was smooth welded-wire mesh designed per ASTM A 185. The available sizes of the welded wires vary from W2.0 thru W8.0 which corresponds to 12.90 mm^2 thru 51.61 mm^2 (0.02 in^2 thru 0.08 in^2). The nominal diameter for each available wire ranged from 4 mm to 8 mm (0.159 in to 0.319 in) and they were typically spaced from 51 mm to 152 mm (2 in to 6 in). The top slab thickness was 191 mm (7½ in) with C_o equal to 51 mm (2 in) and the bottom slab thickness was 152 mm (6 in). The sidewalls were 127 mm (5 in) thick and the haunches extended 127 mm (5 in) from the inside wall and adjacent slab in the horizontal and vertical direction, respectively. A sample design calculation for the top slab of a 1.22 m x 1.22 m x1.22 m (4 ft x 4 ft x 4 ft) box culvert based on LRFD 2004 and interims is presented in Appendix A.

1.3 Literature Review

James (1984) conducted a study to determine the safety of the precast concrete box culverts under the service and design load without the shear connectors. He used 1.52 m (5 ft) and 2.13 m (7 ft) clear span boxes as per ASTM C 850 and applied load on the culvert's span centerline at the supported male end, female end, and the unsupported edge in different tests. This study measured steel stresses and deflections and compared with analytically predicted steel stresses. It was found that the box culvert design is

conservative, and the live load deflections and stresses caused by design service wheel loads are acceptable without shear connectors.

Frederick et al. (1988) conducted theoretical studies, field testing, and model testing. They applied wheel load at center of the 3.66 m (12 ft) and 3.05 m (10 ft) span boxes with and without installed shear connectors. This study reported on the development of a ¼ size laboratory model which was field tested. It was determined that the shear connectors and the edge beams were not required for the ASTM C850 box culverts.

Sonnenberg et al. (2003) conducted thirty - eight concrete specimen tests. It was found that the failure load of the specimens could be predicted using the Mohr-Coulomb theory with an assumed friction angle of 35^0 provided that the normal stress was greater than 0.15 f'_c (concrete cylinder compressive strength). It was concluded that Mohr-Coulomb theory over estimated the shear capacity of the concrete, for normal stresses less than 0.15 f'_c, unless a modified cohesion value and friction angle were used.

McGrath et al. (2004) conducted an analytical study for the Pennsylvania Department of Transportation which investigated the live load distribution widths of reinforced concrete box culverts. The investigation established equations for the distribution of live loads to the top slabs of box culverts with less than 0.61 m (2 ft) of fill using finite element analysis (FEM). The researchers compared the equations in the AASHTO Standards Specifications (AASHTO 2002) to the AASHTO LRFD Specifications (LRFD 2004) and determined that the LRFD Specifications were more

conservative for box culverts, particularly those with spans less than 15 feet. Based on FEM analysis, the researchers recommended new distribution width equations for bending moment and shear and recommended a method of shear transfer between joints.

Yee et al. (2004) investigated and performed load tests on the shear capacity of precast reinforced concrete box culverts. The study concluded that design procedures outlined in both the Canadian Highway and Bridge Design Code (CHBDC) and AASHTO were conservative to a degree. Physical tests confirmed that the computer analysis conducted was reliable for predicting moment distribution widths.

Smeltzer et al. (2004) conducted a study to investigate the safety of precast reinforced concrete box culverts subjected to brittle failure. The researchers concluded that a more thorough evaluation of the shear strength of box culverts should be conducted as well as the establishment of a shear reinforcement requirement.

1.4 Goals and Objectives

The study presented herein was conducted due to the scrutiny of shear capacity in box culverts outlined by previous researchers. The goal of this study was to investigate the shear capacity of box culverts, evaluate existing criteria in the LRFD Specifications, and to provide the data for the development of a parallel analytical model. This report details the load testing procedures, instrumentation and data acquisition systems, results of four load tests, conclusions drawn from the results, and recommendations.

CHAPTER II

TESTING AND INSTRUMENTATION

2.1 Introduction

All analytical structural models are subjected to a specific measure of scrutiny, convergence. Structural models can be deep rooted in theory and thoroughly checked for uniformity; however, if convergence with actual behavior is not achieved, the credibility of the model is forfeited. The focus of the research program discussed herein was to document the behavior of culverts under increasing load and to provide data for the convergence of the proposed analytical model. Several types of data were collected to ensure accuracy. The following chapter details the test setup and the instrumentation system which includes the following items: strain gage instrumentation, laser deflection mapping system, load cell measurement system, analog dial gauge deflection monitoring, hydraulic loading system, data acquisition hardware and software manufactured by instruNet ®, and a laptop computer.

2.2 Load Test Setup

The Structural Testing Laboratory at the University of Texas at Arlington was used to house the load test equipment and to perform tests. Due to the small size of the exterior loading doors, logistics was quickly identified as a critical issue. The two roll-up loading doors were located on the north end of the lab, each providing an 2.44 m (8

ft) wide by 3.05 m (10 ft) tall opening. The available equipment for transporting test culverts was a low capacity forklift. A large steel "A-frame" on casters was created and donated by Hanson Pipe & Products, Inc.® which provided the necessary lifting power and mobility for heavier test culverts. The forklift was utilized for the four tests detailed herein; however, the A-frame was utilized in later tests of larger culverts.

The aforementioned structural laboratory has a strong floor built into its northwest corner. This reaction floor, consists of a five foot thick reinforced concrete slab with two inch diameter anchor holes spaced on 0.61 m (2 ft) centers. A sub floor is located directly below the reaction floor for maintenance and for equipment anchoring. Every hole is designed to comfortably resist an 890 kN (200 kip) pull-out force. The culvert tests discussed herein utilized four load frame columns each having an anchorage pattern of four holes. High strength threaded rods and nuts were used to attach the columns to the reaction floor as shown in Figure 2.1.

Figure 2.1: Load Frame Base

A professional machine moving company was hired at the onset of the project to move the columns into a pre-determined position. The final layout of the load frame is shown in Figure 2.2.

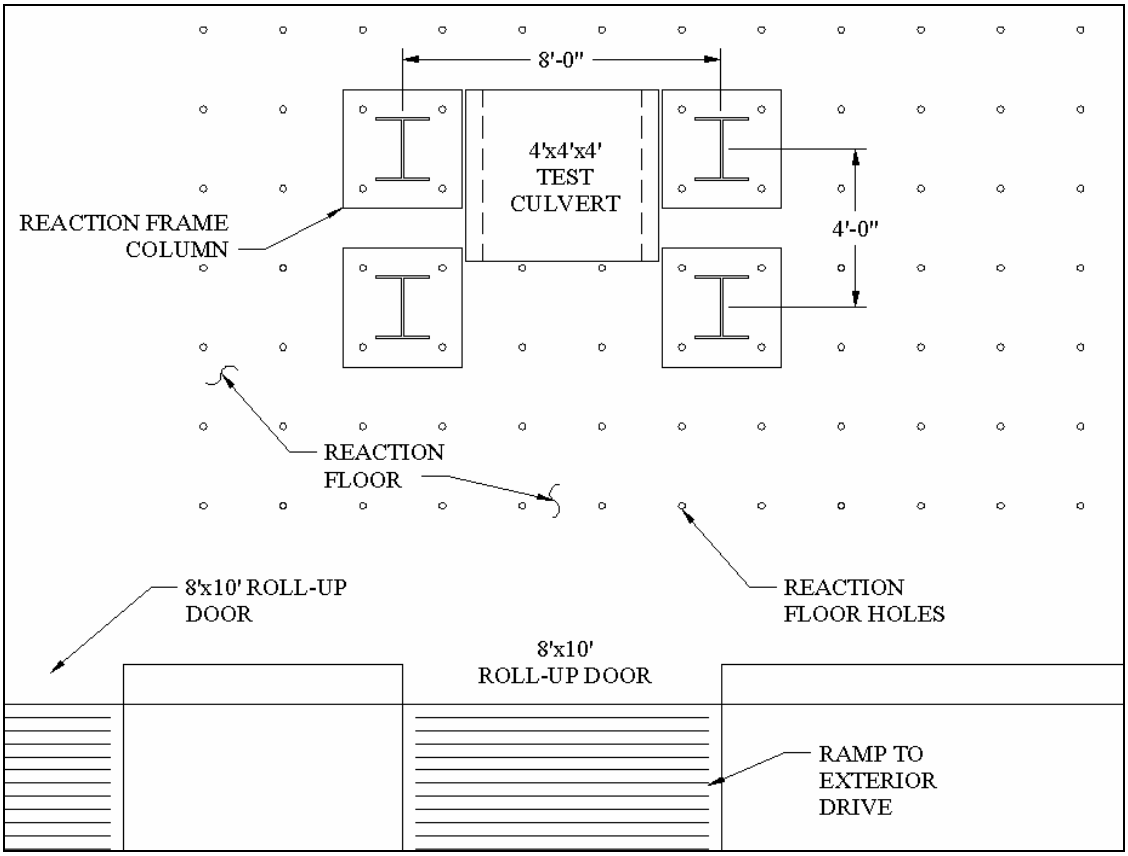

Figure 2.2: Test Floor Layout

Once the load frame columns were in place, a load transfer girder was attached to the four columns. The elevation of the girder relative to the floor was set at approximately thirteen feet to allow clearance for the aforementioned A-frame. Affixed to the bottom flanges of the load transfer girders was an inverted hydraulic jack (see Figure 2.3). The jack was placed in a location along the span that was expected to induce the highest shear stress in the box culvert. The location of the hydraulic jack

was subsequently adjusted prior to each test based on the results of the previous test and early output from the analytical model. A more detailed explanation of this process will be discussed in Chapter 3.

The tests began by placing the culvert in the location shown in Figure 2.2 using the low capacity forklift. Next, the culverts were coated with a white lime treatment, in order to increase the visibility of cracks on the concrete surface during testing (see Figure 2.4). After all physical elements were in place; the instrumentation system was connected and positioned appropriately. Details of the function and position of each piece of instrumentation will be described in section 2.3.

Figure 2.3: Transfer Girder with Hydraulic Jack

Figure 2.4: Lime Treatment

2.3 Instrumentation

2.3.1 Overview

Data was collected in a variety of ways during each load test and details of each system are presented herein. Once the data was collected, it was utilized for the creation and calibration of the analytical model using ABAQUS®. Therefore, the accuracy of the analytical model was directly affected by the quality of the instrumentation system. Figure 2.5 is provided as a reference for this section. The instrumentation of each box culvert included the following: strain gages, laser deflection measurement system, load cell measurement system, hydraulic loading system, data acquisition converter and software manufactured by instruNet®, and a laptop computer.

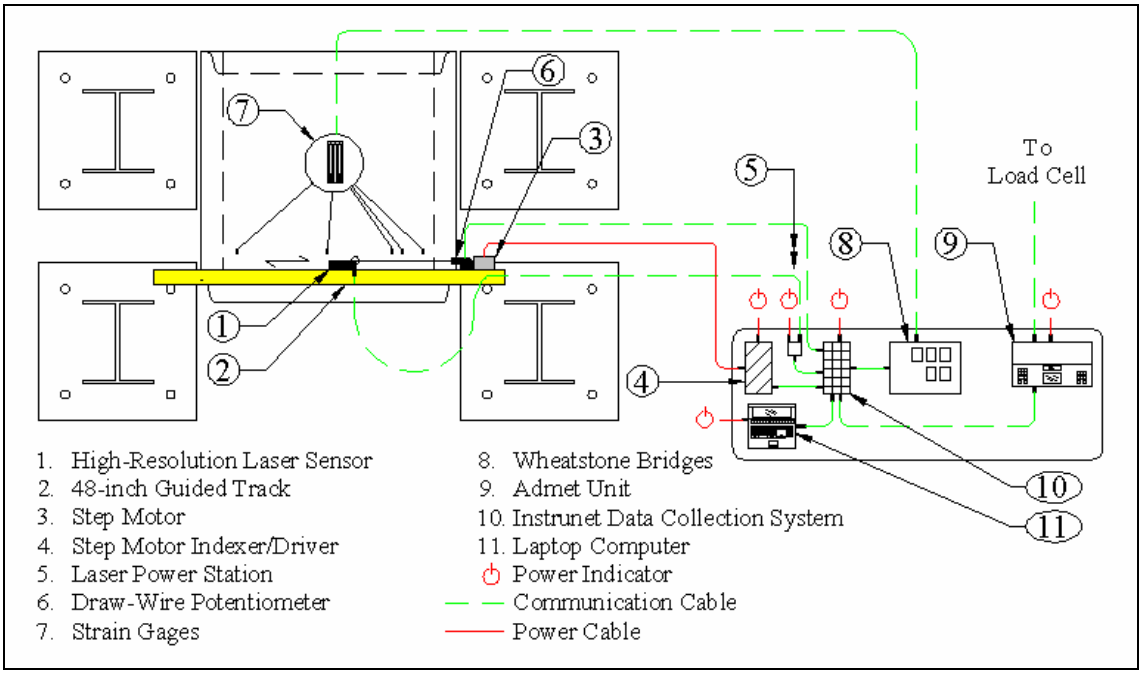

Figure 2.5: Instrumentation Layout

2.3.2 Strain Gage Instrumentation and Casting Process

Each box culvert that was tested contained varying numbers of strain gages placed at critical locations on the steel reinforcement mesh. The application procedure was the most time consuming and delicate task associated with each test. The gages, shown in Figure 2.6, were small and difficult to handle. The selected gage had a constantan 350 Ω grid that was covered with polyimide encapsulation for protection. The range of the gage used was 3.0%, which was substantially more than the range predicted for the reinforcement mesh. The gages and associated equipment were purchased from Vishay Micro-Measurements®, who also recommended application procedures unique to this project.

The process of determining the ideal location for each strain gage was iterative. The gages were designed to measure axial strain in a single direction, so their readings were expected to provide data for bending moments only. Since shear does not act independently, a record of bending behavior would only aid the research effort. Each test culvert had five strain gages applied to their reinforcement, and their locations relative to the span are shown in Figure 2.6. The gages were placed on both the top and bottom layers of reinforcement along the centerline of the 508 mm x 254 mm (20 in x 10 in) loading plate. One gage was placed at each end of the span at the edge of the re-mesh lap in the negative moment region. This location contained the least amount of steel re-mesh, making it a critical location for negative bending stresses. In addition, two gages were placed directly underneath the loading plate. At this location, the span was expected to be in positive bending. However, since the load plate was 254 mm (10 in) wide and positioned close to the wall, the bending behavior of the slab needed to be verified. For this purpose, one gage was placed under the load plate on the top layer of re-mesh to collect data in the case of negative bending and the other on the bottom layer in case of positive bending. The final strain gage was placed at mid-span on the bottom layer of reinforcement.

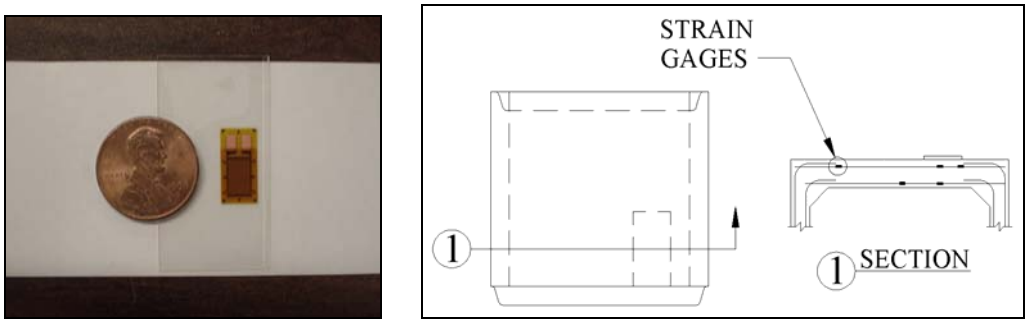

Figure 2.6: Strain Gage and Strain Gage Locations

Once the location for each gage was determined, the gages were applied to the reinforcement mesh. The application process involved the following steps: surface preparation of re-mesh, wet abrasion of re-mesh, placement of gages, soldering and routing of lead wires, and application of a protective coating.

The reinforcement cages were delivered to the University's laboratory in the form in which they were to be cast. The reinforcement generally arrived with a thin layer of rust, which was removed at each gage location using a Dremel ® tool at the onset of surface preparation. Next, chlorinated hydrocarbon degreaser was sprayed on the area and removed using gauze. The degreaser removed general purpose lubricants and hydraulic oils that the reinforcement cage may have been exposed to during fabrication.

The next step in the application process involved wet-abrasion of the reinforcement mesh using a mild phosphoric acid compound and multiple grades of sandpaper. It is important to note that the strain gage application process is a "clean" process, meaning that the slightest amount of particle contamination could produce a faulty bond between the gage and the re-mesh. In order to avoid contamination, each piece of gauze was used only once and was placed in the center of the preparation area and wiped outward toward the undisturbed steel areas. The steel was wiped clean between each cycle of wet-abrasion. In all, three cycles each of 200, 330, and 400 grit sandpaper were performed on each gage location. After wet abrasion was completed, M-Prep Neutralizer 5A was applied to the area to deactivate the M-Prep Conditioner A.

The finished surface was refractory and provided an ideal surface for strain gage bonding.

The third step in the application process utilized M-Bond 200 adhesive to place the strain gage to the re-mesh. The gage was first placed on a piece of cellophane tape with the bonding side open to the air and then was taped onto its desired location. Next, the tape was rolled back exposing the bonding side of the gage and a liquid catalyst was thinly layered onto the gage where it was allowed to dry. Last, a small amount of M-Bond 200 was placed at the base of the tape and the gage was rolled back down onto the steel. While the gage was being placed, a piece of gauze was used to press on the back of the tape in a spreading motion. This procedure ensured that only a very thin layer of adhesive remained between the gage and the prepared surface. The preceding application process was limited to four seconds from the time the catalyst made contact with the adhesive until the bonding adhesive was spread thin. A longer period of time would result in an unusable bond thickness. Pressure was applied to the back of the gage for approximately 90 seconds after placement to allow for the development of a firm bond.

After placement of each gage, the next step involved connecting the communication lead wires to the gages. Each gage contained two enlarged copper soldering tabs that provided a surface for connecting the wires. As an option, soldering terminals were included in the application kit to simplify the soldering process. The terminals were utilized with some gages; however, they did not have an effect on the performance of the gage. As a result, their use is not presented in the data metrics.

Figure 2.7 shows a gage during and after the soldering process without the use of terminals. The wire utilized for this project was carefully selected based on inherent strength and resistance to electric interference. The three-conductor tinned-copper wires were bundled and encapsulated in a protective vinyl jacket to prevent puncture from aggregate impacts during casting. In addition, a braided wire shield was provided around the individually jacketed wires. The shielding served a dual purpose in that it provided additional toughness to the shell of the wire and provided protection from electrical interference. Once attached, the lead wires were routed through the reinforcement cage using small plastic zip-ties. Each wire was routed to the nearest lift hole, which were generally placed in the top slab of precast culverts for ease of lifting during construction. The lift holes are normally cut out of the box after casting; however, for our purposes that method would destroy the wires. Therefore, a four-inch diameter PVC pipe was length-wise cut to the thickness of the top slab and the wires were routed through a small hole on the side the PVC pipe (see Figure 2.8). Each lead wire was labeled using a Post-it® plastic flag to indicate which strain gage location it was connected to. The flags were wrapped several times with cellophane tape to ensure they would not be damaged, faded or accidentally removed during casting. Once labeled, the wires were tied together within the PVC pipe. The ends of the pipe were covered with utility tape prior to casting to prevent the concrete from making contact with and hardening around the free end of the lead wires.

Figure 2.7: Soldering

Figure 2.8: Wire Routing and Protection

The final step in the application process was to apply M-Coat J protective coating to the gage and stripped wire. During the planning stages of this project, protection of the strain gages during casting was a concern. The soldering process alone destroyed multiple gages due to the delicacy of the copper soldering tabs on the gage. Due the aggressive vibration of the casting forms, the moisture in the concrete, and the flow of the concrete material through the reinforcement, the gages needed additional protection. M-Coat J was recommended by the gage manufacturer as an adequate solution. The material was mixed just before it was applied and then allowed

to dry for at least eight hours, depending on the surrounding temperature. Once dry, the coating had a rubberized texture that encapsulated the gage and the stripped wires, protecting them from the harsh casting process (see Figure 2.9).

Figure 2.9: Protective Coating and Casting Process

Once all components of the strain gage application process were performed, the cages were transported to the fabrication plant where they were cast into boxes. The casting process involved a manually operated overhead concrete placement machine and metal form work with an attached vibration motor. Casting typically lasted about five minutes from the placement of the form until the removal of the form. The slump used for the concrete batch was close to 0.0 inches, which allowed the forms to be removed immediately after casting without jeopardizing the structural integrity of the finished product. The target compressive strength for each culvert was 5,000 pounds per square inch. The four test specimens discussed herein were cast on March 24, 2005 in Cedar Hill, Texas.

When the precast culverts had cured to their appropriate strength, the boxes were again transported back to the Structures Laboratory on the University of Texas at Arlington campus. In preparation for each load test, the strain gage wires were guided out of the PVC pipe that was now firmly cast into the top slab of the culvert. Each lead wire was stripped to expose the tinned-copper wires and was then checked using a digital ohm meter. The ohm meter would read a value at or near 350 Ω if the gage survived the casting process. Every box tested herein contained some strain gages that were destroyed during the casting process and some culverts lost all gages. Despite the careful efforts made to protect each gage, either the casting process or the aggressive method of transportation to and from the fabrication plant caused the gages to be rendered unusable. Methods to prevent the loss of strain gages for future tests are discussed in chapter four.

A few strain gages did survive the casting and transportation process. The lead wires associated with the surviving gages were carefully spliced with additional encapsulated lead wires as shown in Figure 2.10. The various layers of the encapsulated wire were stripped down to allow for a good connection. Everyday aluminum foil was used to bridge the braided wire shield, providing the same protection from electrical interference. The splice was then wrapped with electrical tape to hold the connection together in case the wires were accidentally tensioned.

Figure 2.10: Lead Wire Splices

The lead wires for each gage were routed to one of five Wheatstone bridges located on the instrumentation table. The gages had an output of ten volts; however, the Instrunet® system only had a range of five volts. Therefore, the Wheatstone bridges were used to reduce the voltage for input into the instruNet® converter, which will be discussed in detail later in this chapter.

2.3.3 Laser Deflection Measurement System

The top slab deflection profile was measured for each culvert using a traversing optoelectronic deflection sensor. These values were of key importance to the parallel analytical study since all finite element analysis can be broken down into iterations of finite displacements. The setup of the deflection monitoring system was carefully planned in order to ensure the accuracy of the deflection measurements. The laser deflection system consisted of the high-resolution laser sensor, traversing track, step motor indexer/driver, and a retractable draw-wire potentiometer.

The high-resolution laser deflection sensor had a measurement range of 100 mm with a minimum standoff of 50 mm. Its resolution was 20 μm at 1 kHz and it

functioned by reflecting a laser beam off of a target and measured the distance by triangulation (see Figure 2.11). The reflected beam was projected onto a CCD-array element within the unit's casing. The accuracy of the deflection sensor was limited by the surface in which it targeted, in the case of the culvert, a rough concrete surface. This introduced an immeasurable amount of error in the triangulation calculation, as the laser beam may or may not have been projected off of a horizontal surface at any point along the span. To combat this error, a thin strip of metallic tape was placed along the path of the traversing laser. This method of smoothing the surface was ideal since it added no strength to the culvert, deflected uniformly with the culvert slab, and provided a more reflective surface for the laser. Unfortunately, this method proved to magnify the problem because the reflective nature of the metallic strip amplified even the smallest curve on the surface. This can easily be seen in the span vs. deflection plots for tests two and four. Efforts to correct these errors in the data analysis are detailed in chapter three.

The laser sensor was powered by a cable that was directly connected to the unit. The same cable also provided the communication link to the laser power station, which was in turn connected to the instruNet® converter. Details of the data acquisition rate will be discussed later in this chapter.

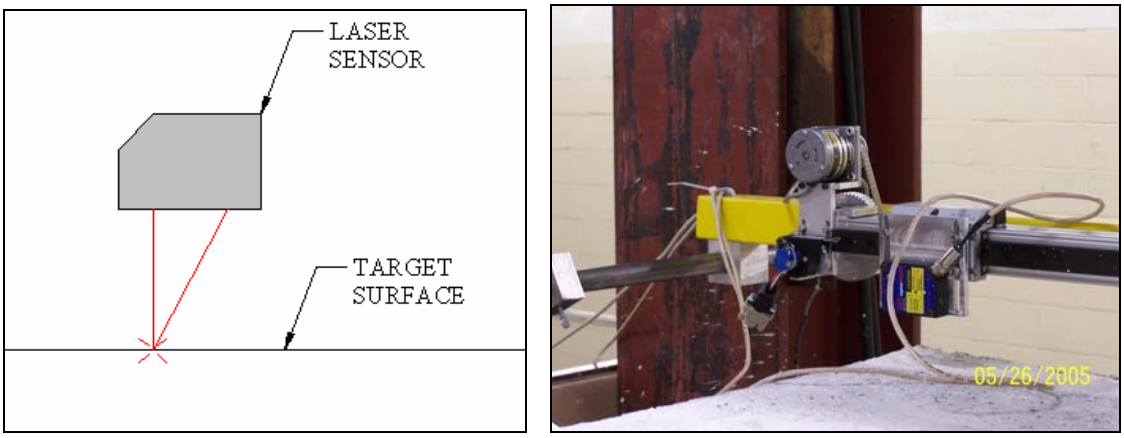

Figure 2.11: Triangulation and Laser Deflection System

The high-resolution laser sensor was mounted to a 48-inch aluminum, single axis motorized stage which allowed it to traverse across the top of the box at a controlled rate. The track was powered by a Compumotor® AX step motor indexer/driver. This device displaced the laser along the track at "snapping" intervals in order to control the rate and provide consistency between tests. The laser took approximately 12 seconds to traverse the full length of the track. The step motor was controlled through the use of computer software installed on the laptop computer.

A draw-wire potentiometer was attached to the stop motor which tracked the distance of the laser along the span. The potentiometer measured with a high level of accuracy and provided a frame of reference for the load vs. deflection plots presented in chapter three. The potentiometer was linked to the Instrunet® controller as input.

In order to ensure the accuracy of the deflection measurements, the laser system had to remain independent of the culvert. This was achieved by attaching support bars between the W12 load frame columns and then spanning a square steel tube member, with the aluminum track attached, over the culvert. The load frame, though stressed

during the test, was being utilized for only 30% of its recommended capacity and a far lower percentage of its ultimate capacity. Therefore, attaching the deflection system to the load frame was not assumed to have significant impact on the measurements. Figure 2.12 shows the laser deflection system in operation.

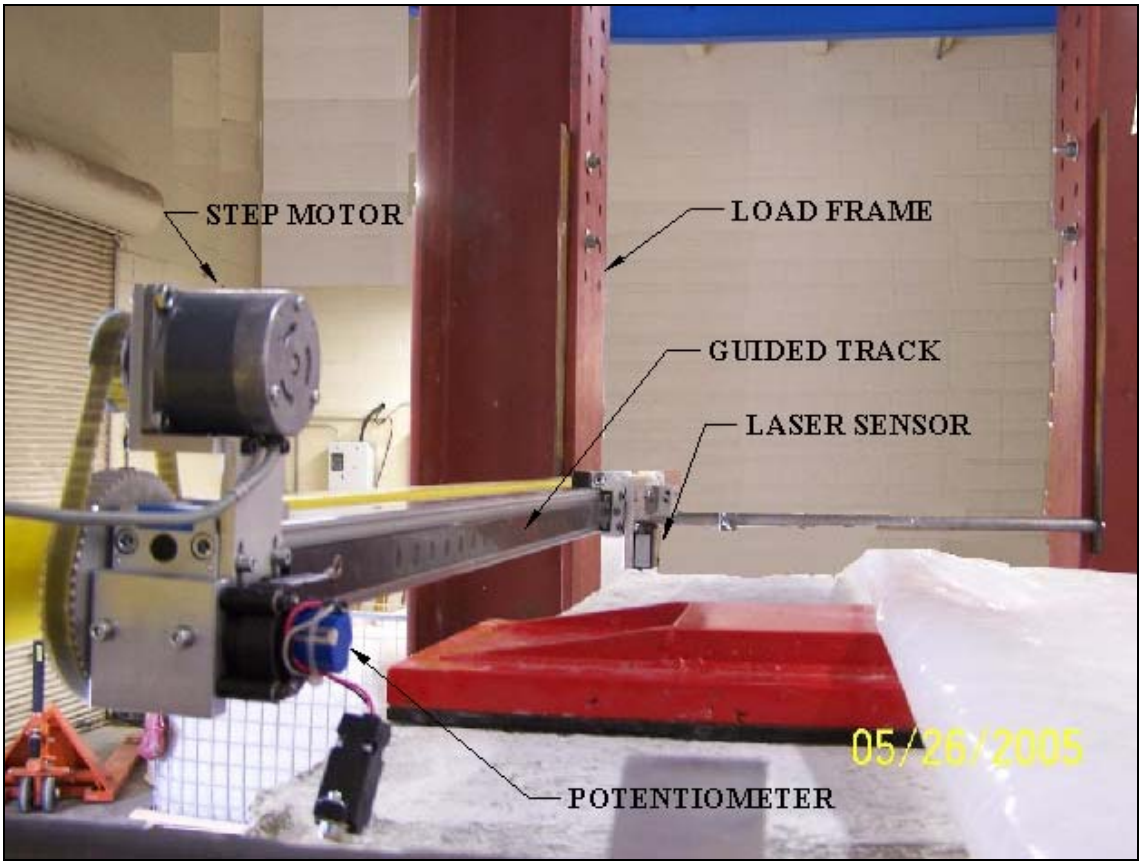

Figure 2.12: Laser Deflection System

2.3.4 Hydraulic Loading System

A hydraulic loading system was used in conjunction with the load frame to test the box culverts. The hydraulic loading system included a hydraulic pressure pump, an inverted hydraulic jack, a load transfer column, and a 508 mm x 254 mm (20 in x 10 in) load plate.

The system was driven by an analog hydraulic pressure pump that was operated through the use of a hand-held controller. It contained an analog pressure gauge that indicated a level of internal pressure in the pump. This pressure was transferred to the inverted hydraulic jack by bleeding a hand operated pressure valve until the desired load was reached. An independent system was used to detect the applied load (see section 2.3.5).

The inverted hydraulic jack was joined to a 24x29.5x2-inch mild steel plate which was attached in soffit to the load transfer girders of the load frame. The jack was used to simulate a HS20 wheel load on top of each test culvert. It had a stroke range of approximately 6½ inches which was well above the anticipated deflection of the culvert. As stated before, the transfer girders were elevated 13-feet above the testing floor. The limited length of the hydraulic jack in the direction of loading made it necessary to utilize a load transfer column to extend to the culvert below. The column was made from a mild steel HSS 4x4x3/16-inch member. The column was welded to an end plate which was clamped to the face of the hydraulic jack using standard C-clamps (see Figure 2.13).

Figure 2.13: Inverted Hydraulic Jack and Transfer Column

Per LRFD Specifications, the loading was spread over an area of 508 mm (20 in) wide by 254 mm (10 in) in the direction of traffic based on standard tire pressure (LRFD 3.6.1.2.5). To achieve this specific contact area, a mild steel plate was designed to transfer the load. A 6.4 mm (¼ in) rubber pad was placed between the load plate and the culvert surface. The pad provided protection from localized stresses beneath the plate and prevented damage to the compression zone of the culvert's top slab during testing.

2.3.5 Load Cell and Admet® Controller

The applied load was measured through the use of a load cell and a controller manufactured by Admet®. The load cell was acquired for this specific purpose and had

a capacity of 890 kN (200 kip), which was higher than the anticipated maximum load of 578 kN (130 kip). The load cell was approximately 114 mm (4½ in) in diameter and approximately 152 mm (6 in) tall. The top of the load cell utilized a rounded button to ensure that the load was passed through a point and not spread out over an area. In order to measure the load accurately, the load cell was placed directly on the load plate. This ensured that the load cell would capture not only the applied load, but also the self-weight of the loading components above. A self-leveler was placed between the load cell and the load transfer column to transfer the load vertically to the top of the culvert. The load cell was connected to the Admet® controller by a single cable housing both communication and power leads.

The Admet® controller was a multifaceted testing device; however, this project only used the unit as a means of communication with the load cell. The digital display on the front of the controller allowed the load to be read dynamically to a high level of precision during the test. In addition to the visual display, the controller output the load measurements to the Instrunet® data acquisition system to be described in section 2.3.6.

The load cell and Admet® controller were professionally calibrated and internally tested to ensure the accuracy of the load measurement. Taking all system errors into account, the load was measured within a range of one to two percent. Figure 2.14 displays the load cell, self-leveler and Admet® controller.

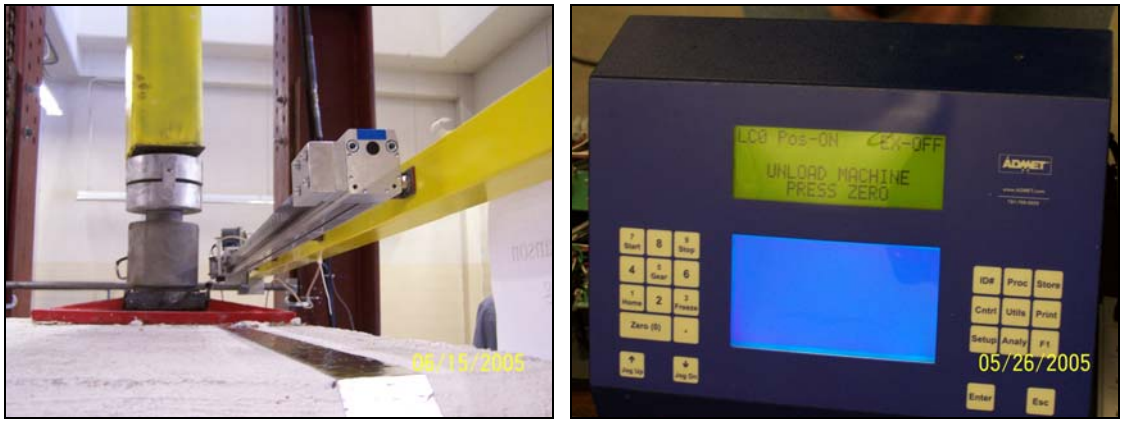

Figure 2.14: Load Cell, Self-Leveler and Admet® Controller

2.3.6 instruNet® Converter Data Acquisition System

The data acquisition system used for this project was a multi-channel converter device manufactured by instruNet® (see Figure 2.15). The instruNet® converter contained 32 channels in a daisy-chain configuration for input, and of those, eight were utilized for the culvert tests. The converter board was equipped with its own microprocessor and on board RAM to handle the various loads of information passed through it. It was capable of receiving digital and voltage input and converting it to usable computer data. The output from the system was transferred to a laptop computer through the use of a pc card.

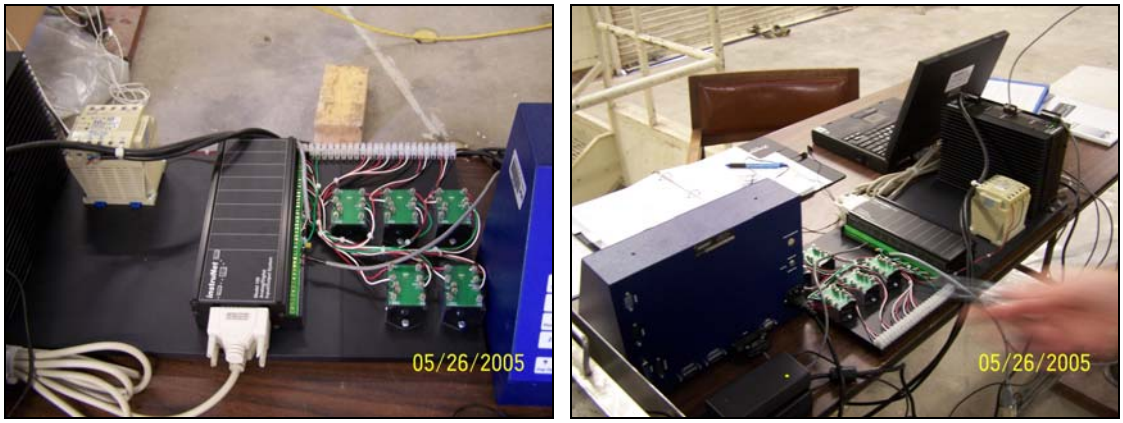

Figure 2.15: instruNet® Converter Board and Laptop Computer

The laptop computer contained preinstalled instruNet® World software that was capable of recording input from all 32 channels of the converter board. The software interface (see Figure 2.16) provided a means to manage, monitor, and operate the data acquisition system. For the culvert tests, the program recorded data at a predetermined rate of 0.12 seconds per interval. The measured variables for the instruNet® World program were time (measured in seconds), applied load (load cell and Admet® controller), reinforcement strains (up to five strain gages), laser position along the span (potentiometer output), and culvert top slab deflection (high-resolution laser sensor). The software provided the option for binary or wave format text files as output. The wave files were used in this study and were transported to Microsoft® Excel for data analysis.

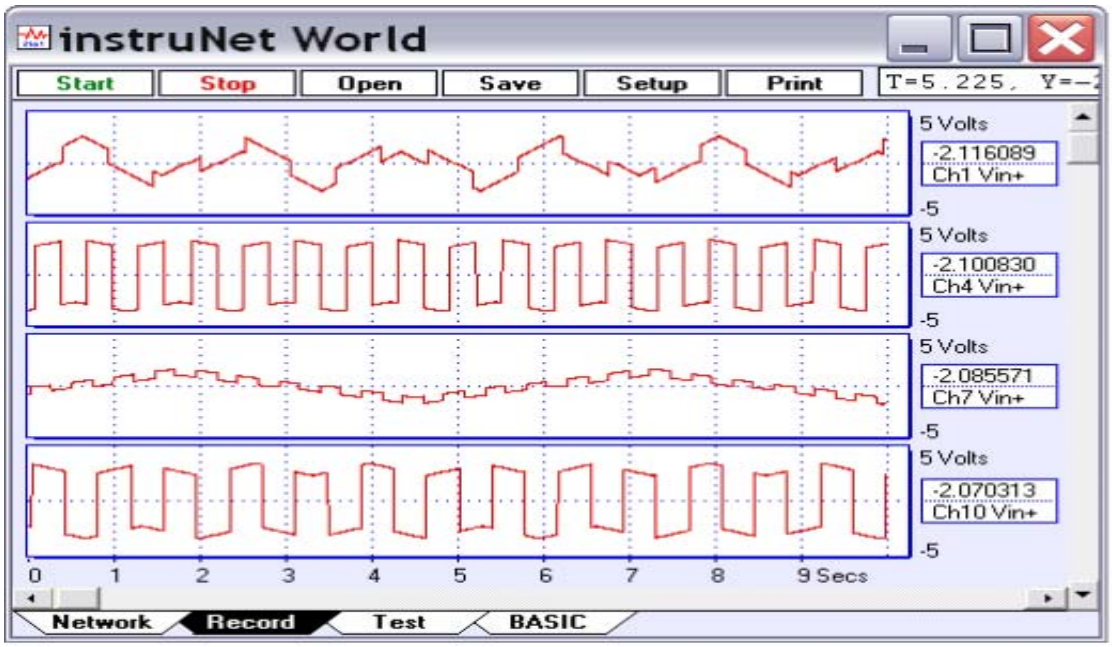

Figure 2.16: instruNet® World Software Interface

2.3.7 Load Test Procedure

Prior to each test, a culvert was placed into its predetermined position, white washed with lime treatment, and connected to all applicable instrumentation systems as described in previous sections. Each research team member and spectator was provided with the appropriate safety equipment prior to the start of testing. Once all systems were functioning properly, the test was ready to begin.

Each test commenced by taking a traversing laser deflection measurement with no load applied. This measurement served as the baseline for all further deflection readings. Loading was applied to the culvert and data acquisition readings were recorded dynamically as the load increased. Once the load reached the target interval, the data acquisition system recorded a separate output file, while the laser deflection

system traversed across the span. Once the laser had traversed, the system was unloaded back to zero while the data acquisition system recorded a third string of data. This process was repeated at load increments of 5 kip until the first flexural cracks appeared. The loading and unloading measurements provided residual deflection data for the parallel analytical model. Once cracking occurred, the process above was repeated at varying load intervals; however, the system was no longer unloaded back to zero. Each culvert was tested to ultimate failure which was determined when the culvert could no longer carry additional load. Figure 2.17 shows a typical load history for each test.

Throughout each test, cracks were recorded using three different methods. First, a permanent marker was used to sketch a line parallel to the actual crack for visibility in photographs. A perpendicular line was drawn at the end of the crack indicating the end of propagation. Additionally, the load increment at which the fracture occurred was written next to the perpendicular line to provide a frame of reference for propagation at higher loads (see Figure 2.18). Secondly, photographs were taken throughout the test to provide visual records. The last method of recording crack propagation involved a written log. Each entry included a description of crack width, location, load increment at which the fracture occurred, and the type of crack (flexure or shear). Details of the crack propagation for each test are presented in chapter three.

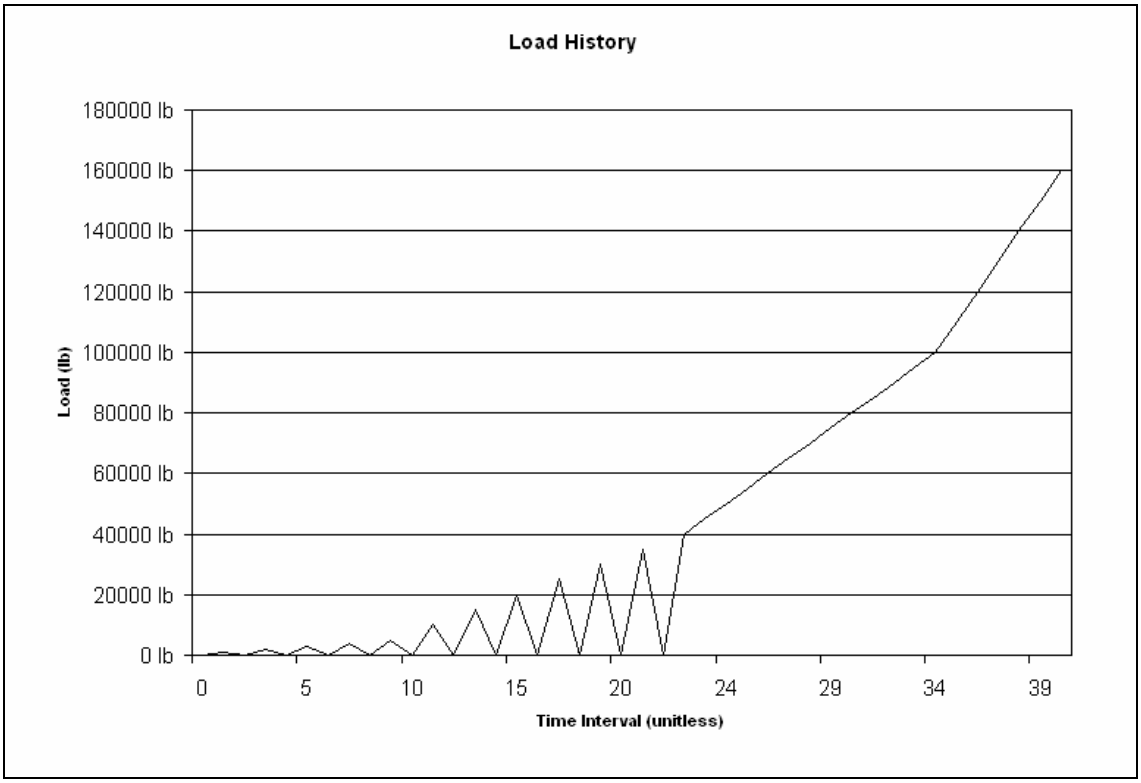

Figure 2.17: Typical Load History

Figure 2.18: Crack Propagation

CHAPTER III

LOAD TEST RESULTS AND COMPARISONS

3.1 Introduction

Results and comparisons of physical load tests performed on four precast concrete box culverts are presented herein. Included in the results for each culvert are crack development, deflection measurements and comparisons, load vs. deflections plots, and comparisons with requirements of AASHTO LRFD specifications.

The size designation of each box was 4 ft x 4 ft x 4 ft, corresponding to the span, rise and joint length respectively. The following labeling system was used to describe each test culvert: S or B-S or DB-SRL-NB or WB-P where acronyms are as follows:

S – Spigot end

B – Bell end

SB – Single box culvert

DB – Double box culvert

SRL – Dimensions of the culvert [Span (ft), rise (ft), and joint length (ft)]

NB – No bedding

WB – With bedding

P – Distance from inside edge of adjacent haunch to the center of the loading plate (in) (O in Table 4.2 indicates a value that is to be optimized through FEM analysis)

For instance, test number 1 is annotated as S-SB-444-WB-5 because the load was applied to the spigot end; a single box was tested; it had a 4 ft span, 4 ft rise, and 4 ft joint length; bedding material was used; and the center of the loading plate was placed 5 in from the inside edge of the adjacent haunch.

Table 3.1 details the variable instrumentation and test setup conditions that were applicable to each of the four tests. The error associated with each test was distinctly different based on the testing conditions. Therefore, it is important to note the information in the following table when comparing results.

Table 3.1: Variable Instrumentation and Test Setup Conditions

Test Designation	Traversing Laser	Strain Gages	Bedding
S-SB-444-WB-5	X	3	X
S-SB-444-NB-5	X	-	-
S-SB-444-NB-6$^1/_2$	-	-	-
S-SB-444-NB-11$^1/_2$	X	3	-

The parallel analytical model sought convergence through comparison with test data obtained from the culverts discussed herein. As stated before, the model was developed using ABAQUS® finite element software which uses finite displacements to calculate stresses on defined elements. Span vs. deflection profiles and load vs. maximum deflection curves are provided for each culvert as a basis for the convergence of the analytical model.

The results of each test were compared with the AASHTO LRFD Bridge Design Specifications for adherence to the provisions for service live load deflection, crack control, and shear capacity. A standard HS20-44 design truck is used as the basis of design for concrete box culverts with less than 0.61 m (2 ft) of fill material. Therefore,

a 71.2 kN (16 kip) wheel load is the governing service live load for a culvert with a joint length of 1.22 m (4 ft) (LRFD 2005, 3.6.1.3.3). The service live load deflection induced by the wheel load is limited to L/800 or 1.52 mm (0.06 in) for a 1.22 m (4 ft) span (LRFD 2005, 2.5.2.6.2). The crack width limitation was set at 0.33 mm (0.013 in) (LRFD 2006, 5.7.3.4). The required shear capacity is based on a factored live load plus dynamic load allowance and multiple presence factor equal to 198.8 kN (44.7 kip) (LRFD 2006, 2004 & 2005, Tables 3.4.1-1, 3.6.1.1.2-1 & 3.6.2.1-1).

3.2 Load Test Number One: S-SB-444-WB-5

3.2.1 Test Overview

Load test number one was performed on June 2, 2005 in the structural laboratory at the University of Texas at Arlington. The test utilized a three-inch layer of ¾-inch graded stone aggregate as bedding material. This bedding was intended to simulate in-service support conditions; however, no provisions were made to mimic lateral earth pressure on the walls of the culvert. Three of the five strain gages that were installed on the reinforcement cage survived the casting process. The data obtained from the three strain gages was inconclusive and has been omitted from the contents of this paper. Recommendations for future use of strain gages are provided in chapter four. All other instrumentation systems were fully functional during the test. The center of the loading plate was placed on the spigot end of the culvert, exactly five-inches from the inside edge of the adjacent haunch. The concrete compressive strength for this culvert, as measured from a cylinder break on the day of the test, was 8,500 psi. This value was higher than the design compressive strength of 5,000 psi.

3.2.2 Crack Propagation

During test 1, hairline flexure cracks first appeared on the top of the bottom slab directly beneath the load plate around 156 kN (35 kip). Another flexure crack appeared near the same location at 208 kN (40 kip). Both cracks were visible, but less than the 0.33 mm (0.013 in) crack control limit set by AASHTO. Propagation of these cracks and other hairline cracks on the top slab continued to develop until a 415 kN (80 kip) load was reached. At this load increment, the first shear crack developed at the tip of the haunch adjacent to the load plate. Flexure cracks spanning the entire joint length of the culvert developed on the outside of each wall around 467 kN (90 kip). At 493 kN (95 kip), a shear crack extended from the edge of the load plate towards mid-span. Other less significant cracks formed and propagated until the conclusion of the test. The culvert failed in flexure at a load of 534 kN (120 kip) when the culvert continued to deflect without increasing load. After failure had been declared, the sidewall adjacent to the load fractured diagonally as additional load was applied. Figure 3.1 provides pictures of each face of the culvert after failure.

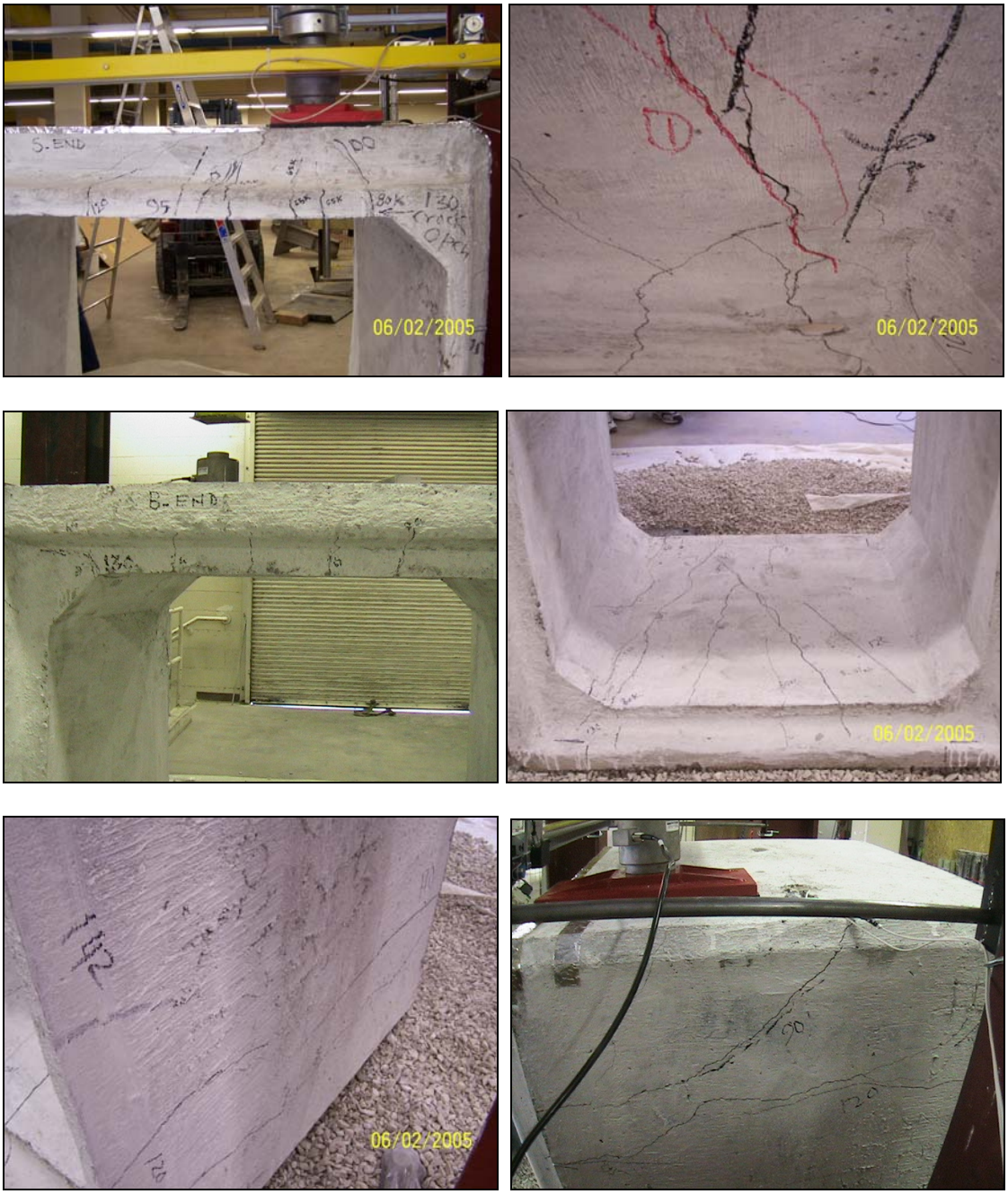

Figure 3.1: Test One Failure

3.2.3 Bedding Correction and Deflection Curves

The bedding material that was used in test 1 was unrestrained against spreading; therefore, the box was allowed to settle into the material. Under in-service conditions the bedding material would be held into place by surrounding pressures, reducing the amount of global settlement. The load was placed near a corner on the top slab, which caused differential settlement between the four corners. The corner opposite of the load experienced the least amount of settlement, while the corner under the load experienced the most. In addition, the high stress concentrations below the loaded corner caused some of the aggregate to be crushed (see Figure 3.2).

Figure 3.2: Bedding Settlement and Crushed Aggregate

The deflection measurements were taken independently of the culvert's settlement; therefore, the bedding material introduced error into the top slab deflection measurements. Figure 3.3 depicts the span vs. deflection profile as it was measured. This profile reflects both the differential settlement of the culvert through the bedding and the deflection of the top slab at various load intervals.

In order to determine the structural behavior of the culvert, the differential settlement caused by the bedding material had to be subtracted from the raw data. This data was important for the parallel analytical model because the deflection of the top slab was a function of the culvert's structural integrity and not the support condition. In addition, the other tests were performed without bedding material, so it was necessary to modify the data for comparison purposes. The laser data for test number one produced a smooth profile, allowing for a higher level of accuracy when determining the bedding material's differential settlement. The settlement was proportional to the load applied; therefore, delta values corresponding to the bedding settlement were calculated for each load increment (see Figure 3.3). The two delta values at either end of the span were used to produce a linear profile representing the differential settlement of the bedding material. These profiles were subtracted from the original profiles for each load increment (shown in Figure 3.4) to produce the span vs. deflection graph presented in Figure 3.5. Additionally, the deflection at the load plate is provided in Figure 3.6. A load vs. deflection graph is provided as reference for the parallel analytical model in Figure 3.7. The values for Figures 3.6 and 3.7 were measured at the mid-span edge of the load plate.

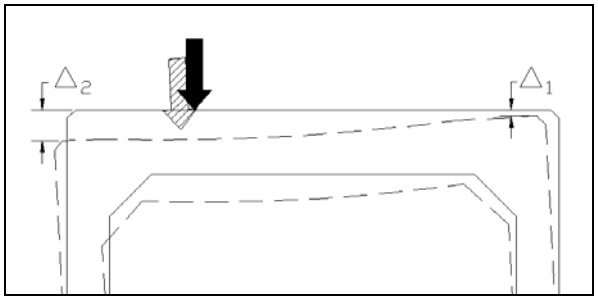

Figure 3.3: Differential Settlement

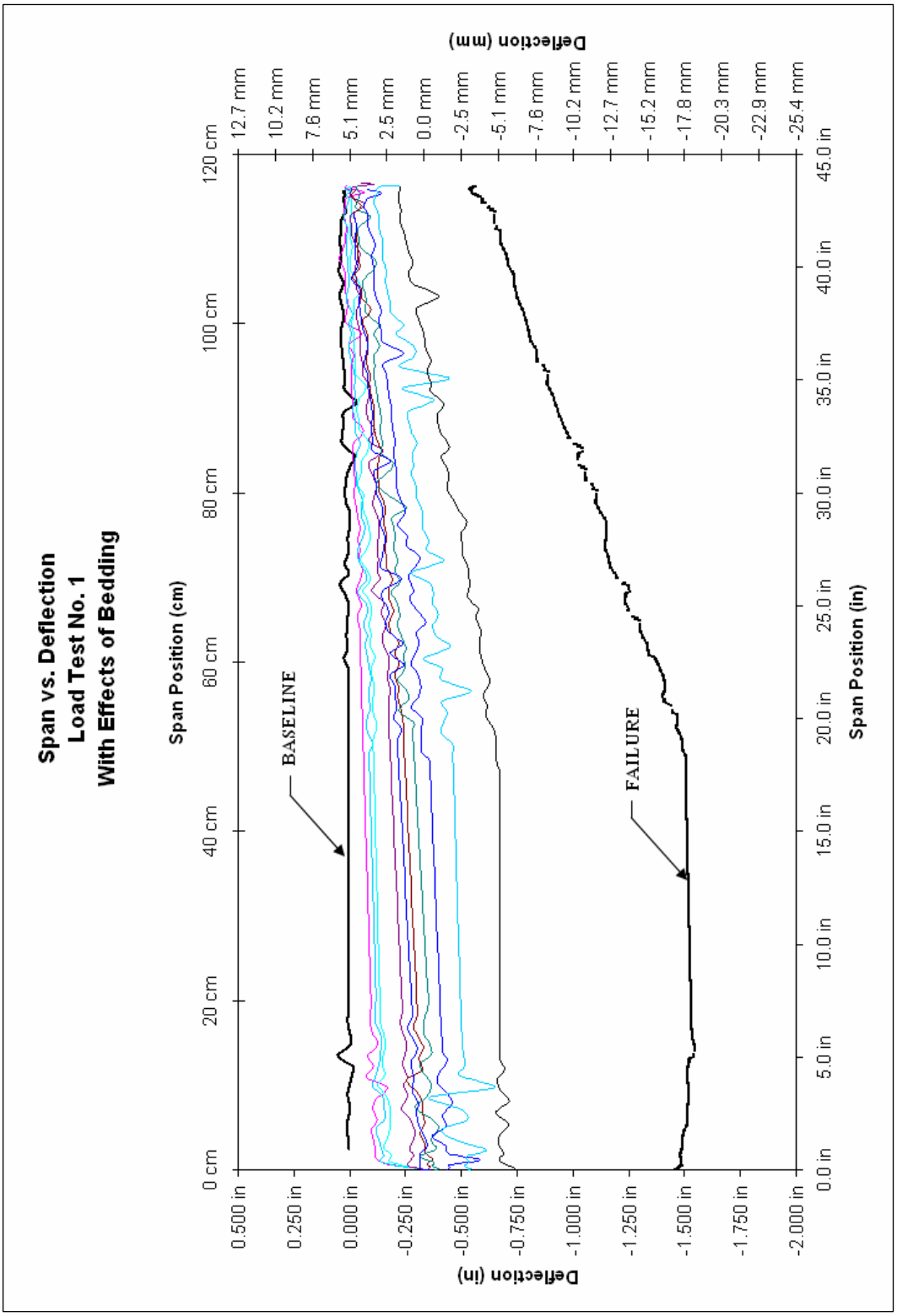

Figure 3.4: Span vs. Deflection with Effects of Bedding

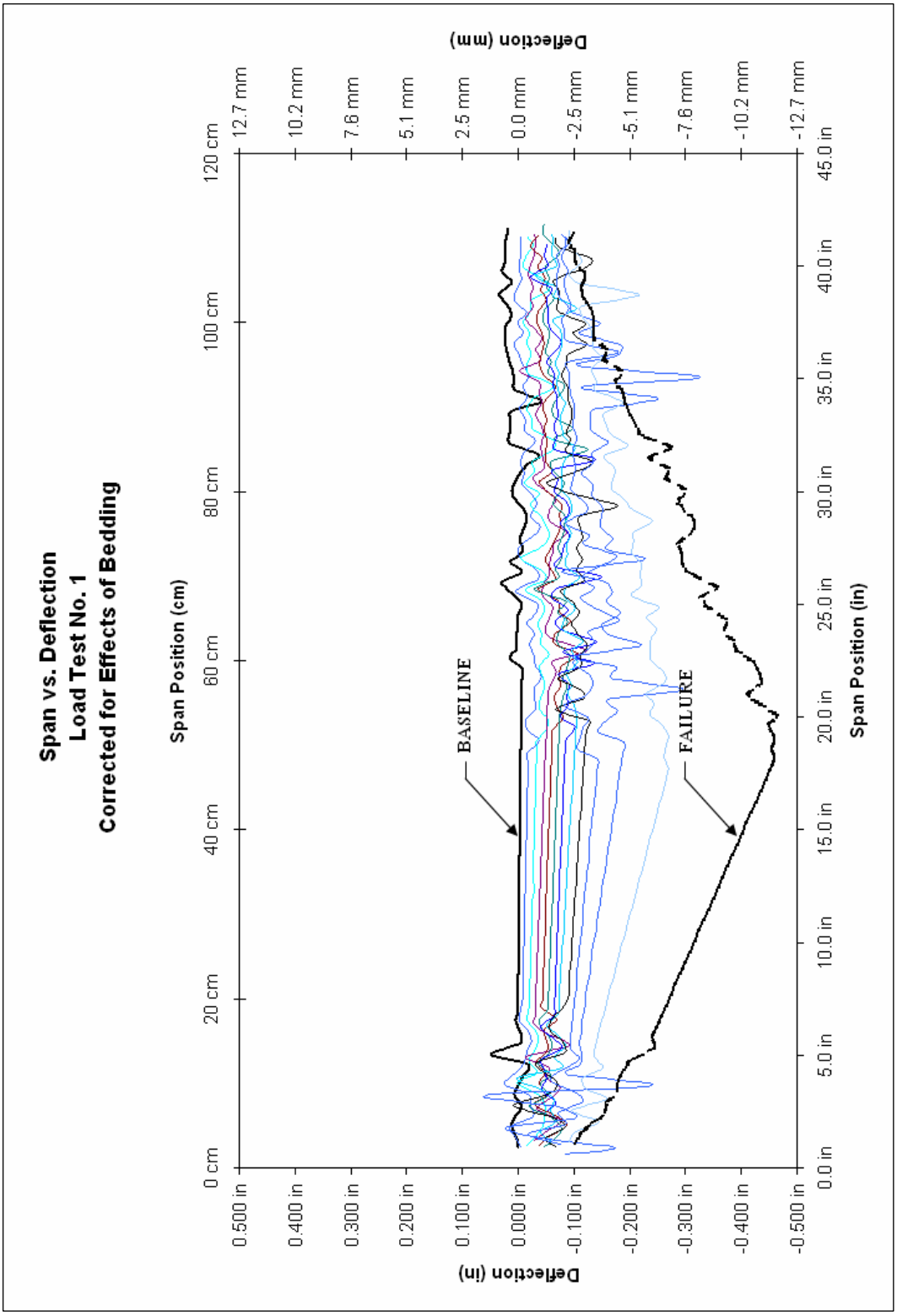

Figure 3.5: Span vs. Deflection Corrected for Effects of Bedding

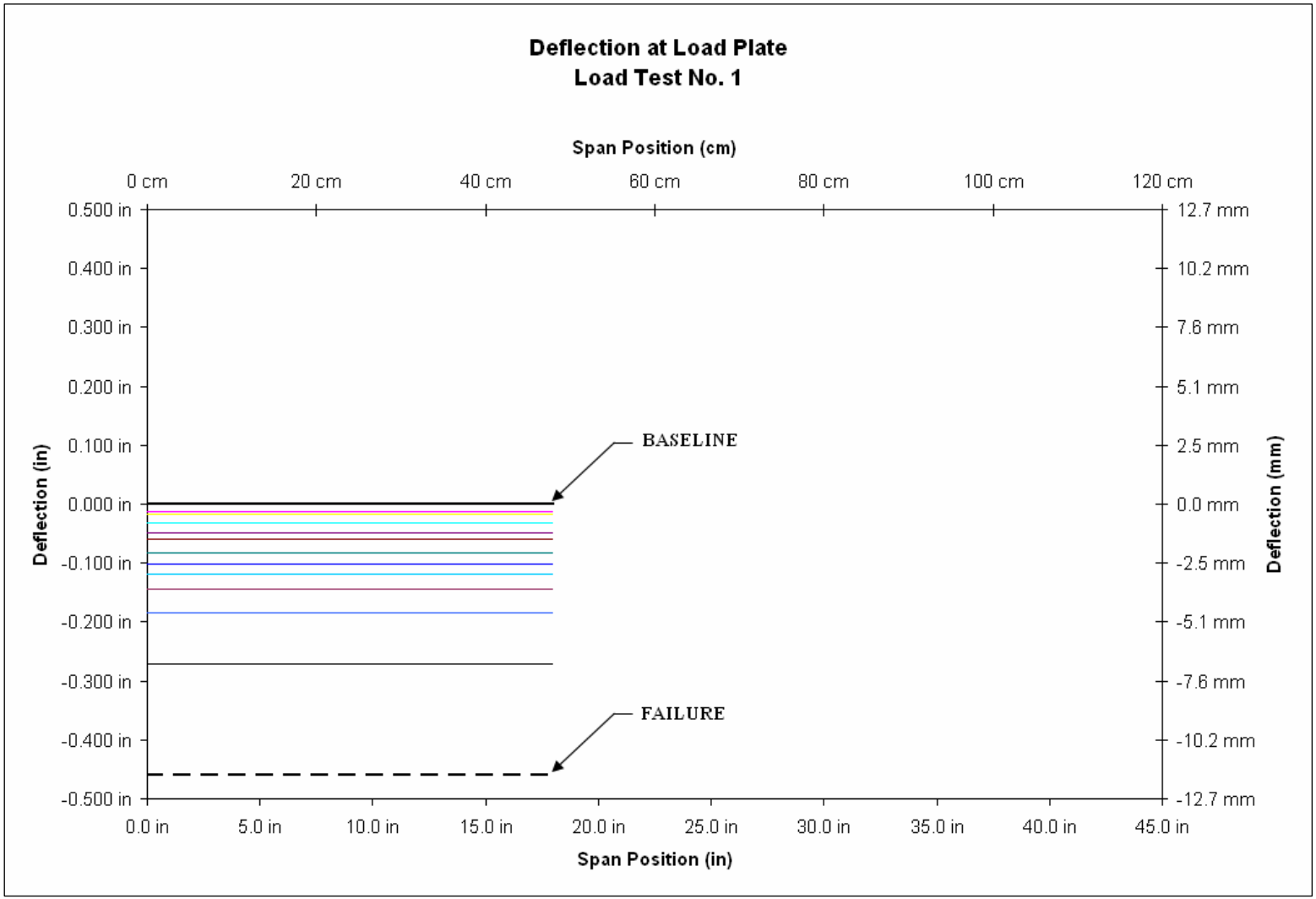

Figure 3.6: Deflection at Load Plate Corrected for Effects of Bedding

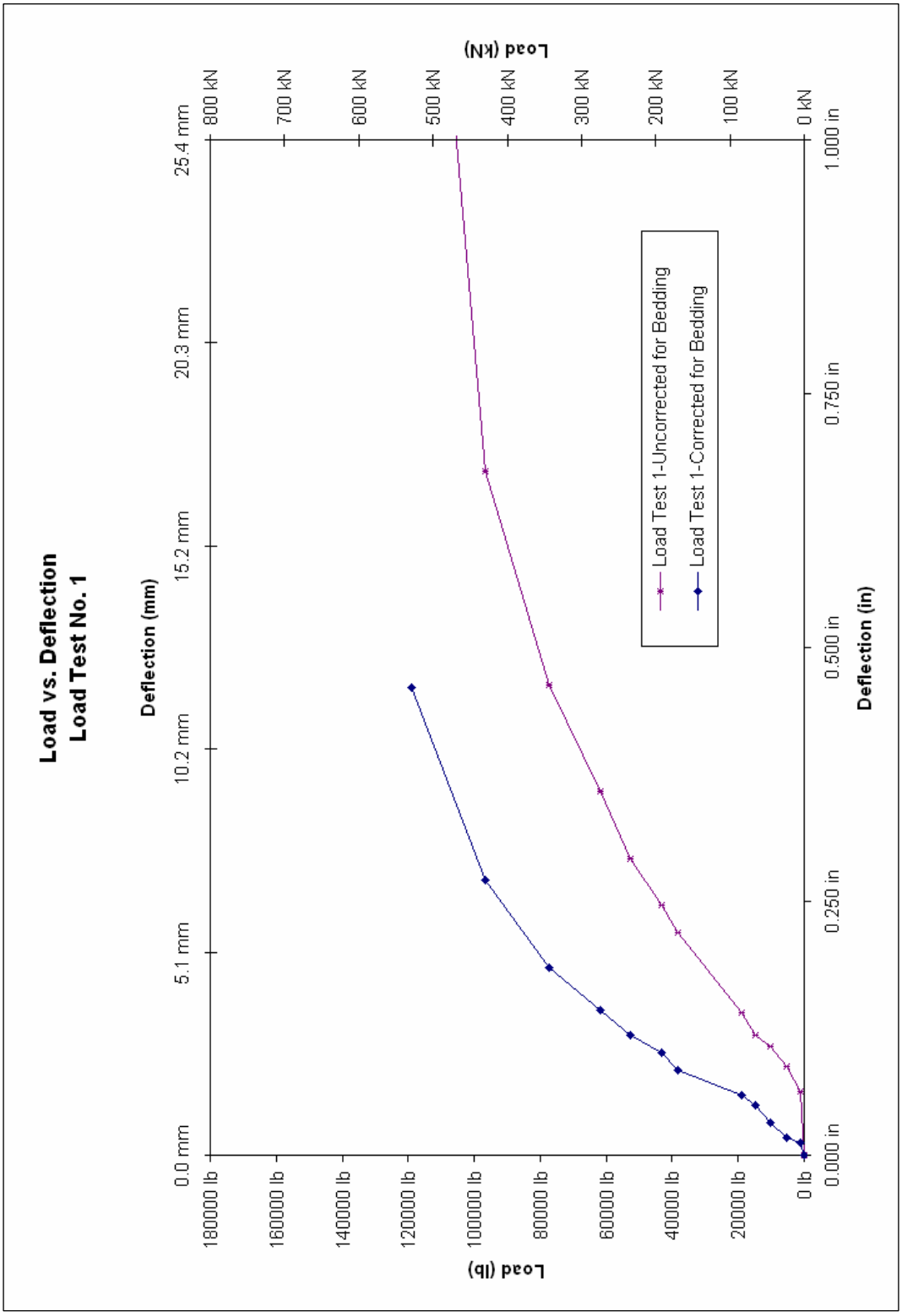

Figure 3.7: Load vs. Deflection

3.2.4 AASHTO Comparisons

The first crack exceeding the AASHTO LRFD width limit of 0.33 mm (0.013 in) occurred in flexure around 356 kN (80 kip). A shear crack exceeding the limit occurred at 423 kN (95 kip).

The maximum deflection value was taken from the laser deflection profile at the mid-span edge of the load plate (see Figure 3.6). Deflection readings used for comparison purposes were modified using the bedding correction method detailed in section 3.2.3. The maximum deflection at the 67 kN (15 kip) load increment was approximately 1.24 mm (0.05 in), which is less than the allowable limit. It can be determined by interpolation with the 89 kN (20 kip) load increment that the deflection at the 71 kN (16 kip) service load was less than 1.52 mm (0.06 in), although measurements at 71 kN (16 kip) were not recorded. Figure 3.8 shows the deflection of the load plate for the 67 kN (15 kip) load increment along with the AASHTO limit and the baseline.

The shear failure, which commenced after flexural failure was declared, occurred at approximately 534 kN (120 kip) which is well above the calculated value of 230 kN (51.7 kip). Calculations for shear capacity based on the AASHTO LRFD Specifications (LRFD 5.8.3.3) are provided below. The calculations will be utilized in the AASHTO Comparisons section for each load test; however, only the resulting capacity will be presented hereafter.

$$V_n = V_c + V_s + V_p (V_s = 0; V_p = 0)$$

$$V_n = V_c = 0.0316\beta\sqrt{f'_c}\, b_v d_v = 0.0316(2.0)\sqrt{8.5}(48)5.85 = 51.7kip << 120kip$$

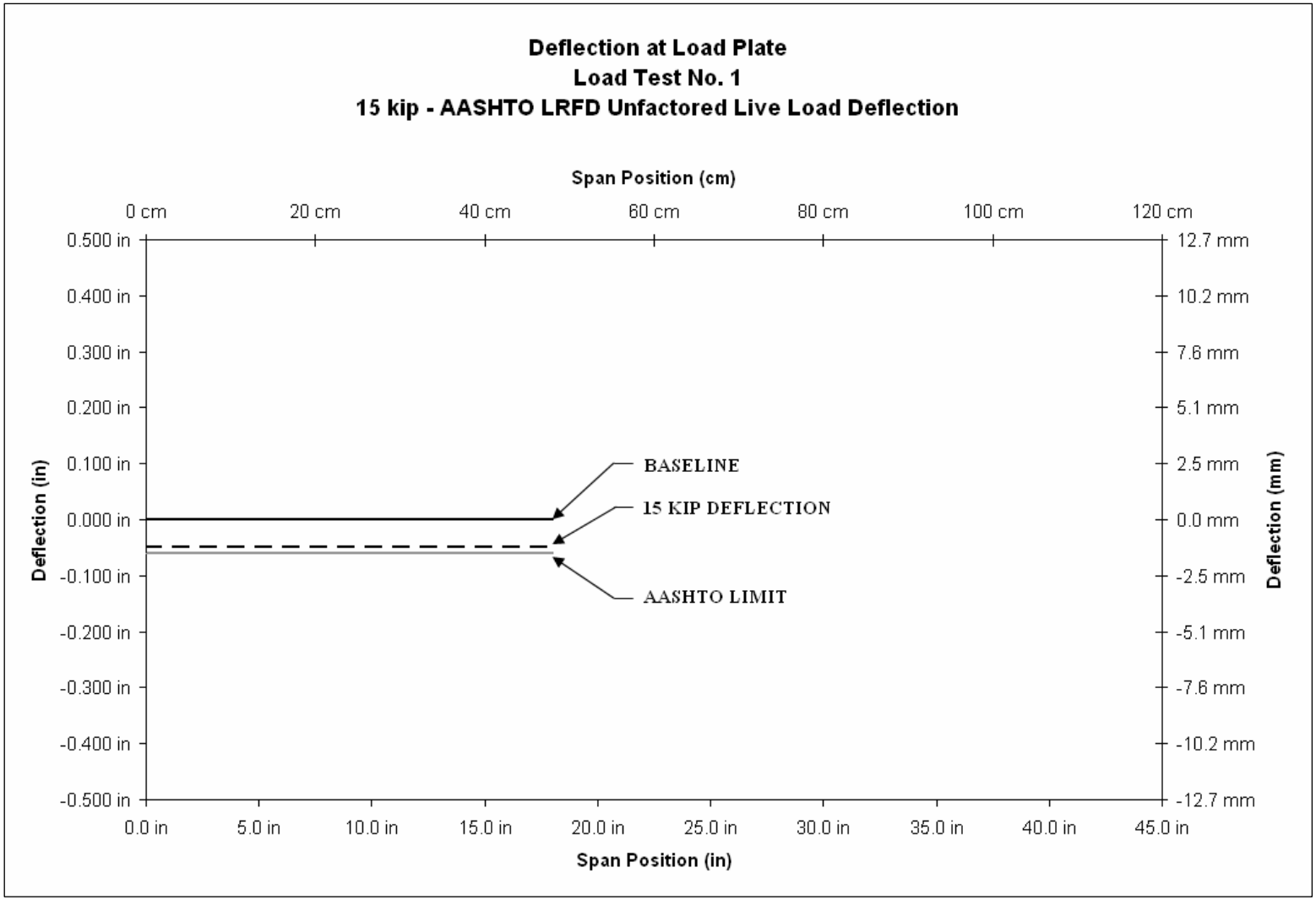

Figure 3.8: Deflection at Load Plate AASHTO Deflection Limit

3.3 Load Test Number Two: S-SB-444-NB-5

3.3.1 Test Overview

Load test number two was performed on June 15, 2005. Unlike test 1, no bedding material was placed under the culvert. This provided a more accurate measurement of the top slab deflection. None of the five applied strain gages survived the casting process. All other instrumentation systems were fully functional during the test. Metallic tape was placed on top of the culvert during test 1. The center of the loading plate was placed on the spigot end of the culvert, exactly five-inches from the inside edge of the adjacent haunch. The concrete compressive strength was determined by testing to be 8,500 psi, which was higher than the 5,000 psi design strength.

3.3.2 Crack Propagation

The first visible cracks were flexure cracks located on the bottom of the top slab and top of the bottom slab at 133 kN (30 kip). These cracks continued to widen and propagate until a 267 kN (60 kip). At that load, hairline flexure cracks, smaller than the 0.33 mm (0.013 in) limit, developed along the outside of the culvert walls. The first shear crack occurred at the spigot end near the adjacent wall at a load of 267 kN (60 kip). The shear crack spread to the bell end between 267 kN and 334 kN (60 kip and 75 kip). The flexure cracks along the sidewalls extended the full joint length from 334 kN to 512 kN (75 kip to 115 kip). Another shear crack developed on the mid-span side of the load plate at 512 kN (115 kip). Prior cracks continued to propagate and others continued to form until the ultimate failure load of 712 kN (160 kip) was reached. The

culvert failed in shear along around the load plate. Figure 3.9 provides pictures of each face of the culvert after failure.

Figure 3.9: Test Two Failure

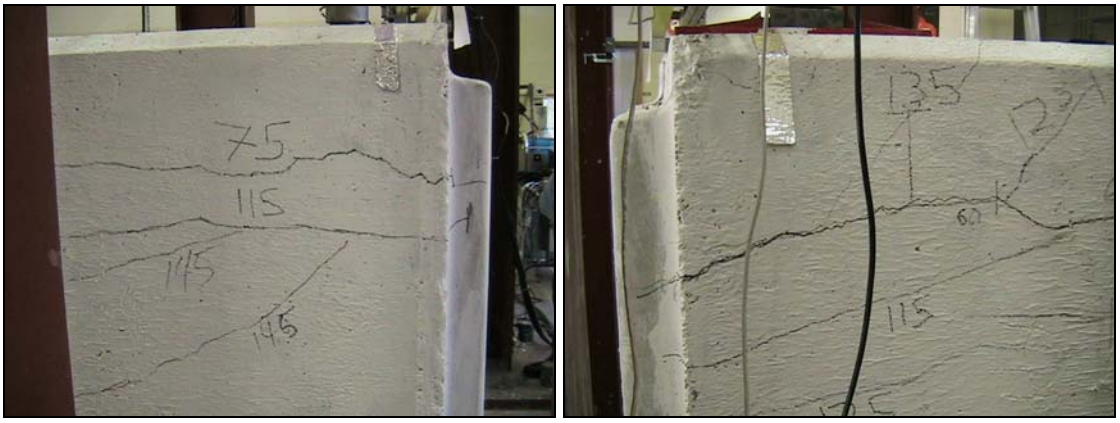

Figure 3.10: Test Two Failure

3.3.3 Deflection Curves

The culvert deflected in a similar manner to the first test; however, the lack of bedding material provided a more realistic measurement of the culvert's structural integrity. The metallic tape beneath the laser sensor caused the deflection profile data to be inconsistent along the span. Unlike the rest of the span, the data at the load plate was smooth and useful, so the deflection at the mid-span edge of the load plate is presented in lieu of a span vs. deflection graph (see Figure 3.10). Additionally, a load vs. deflection graph at the load plate is provided as reference for the analytical model (see Figure 3.11).

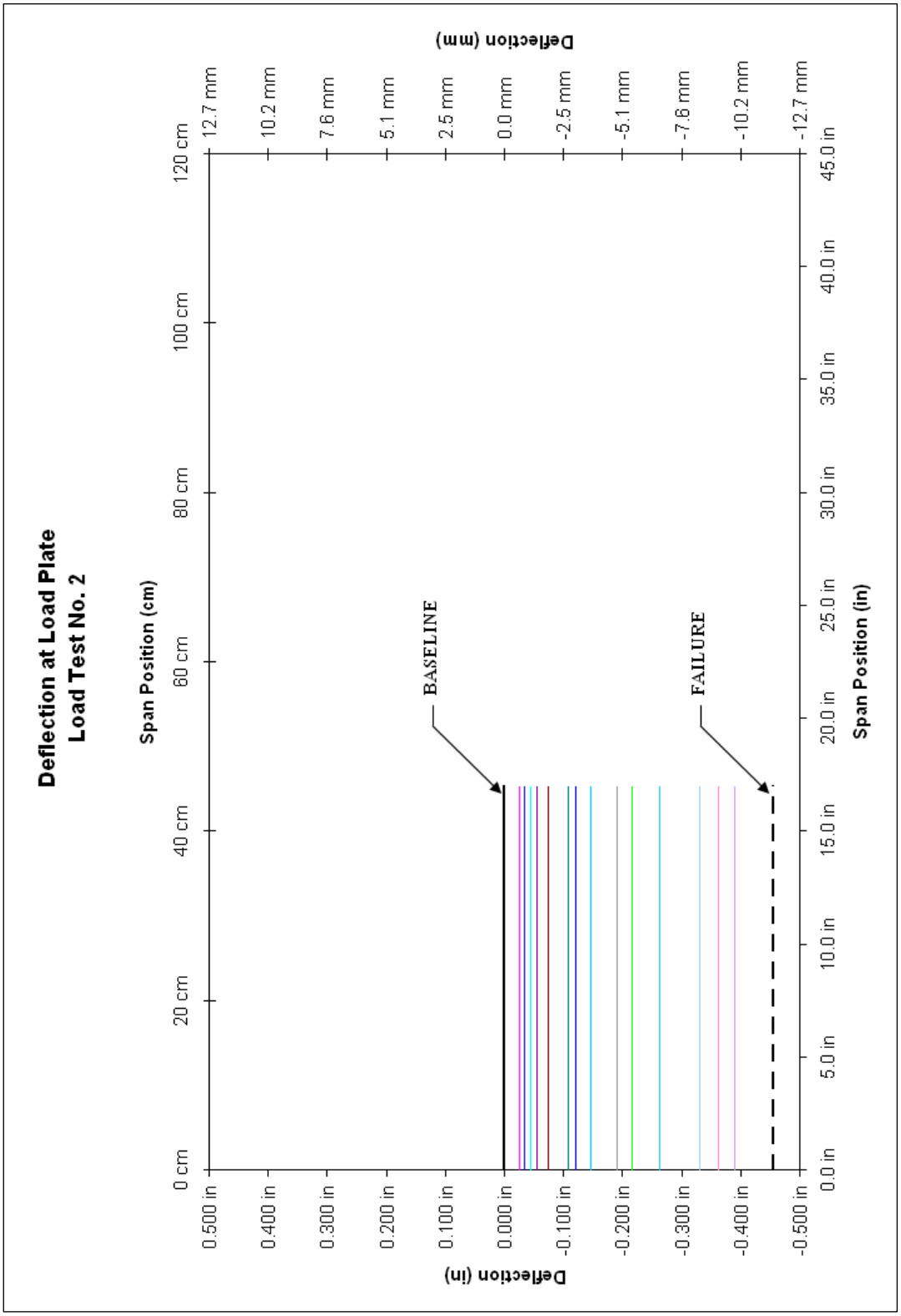

Figure 3.11: Deflection at Load Plate

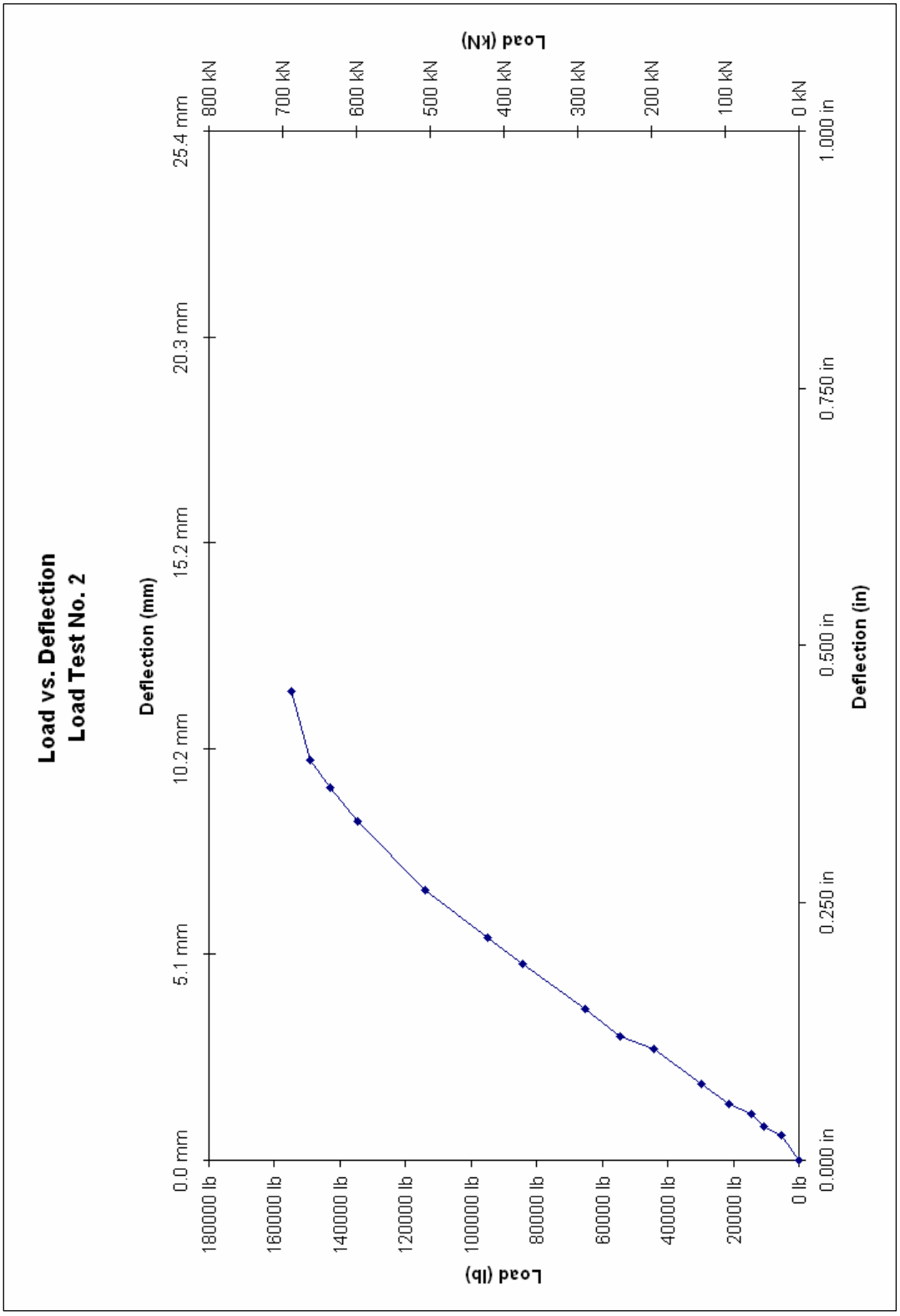

Figure 3.12: Load vs. Deflection

3.3.4 AASHTO Comparisons

During test 1, the first crack to exceed the 0.33 mm (0.013 in) width requirement occurred in flexure at 222 kN (50 kip). The first shear crack to exceed the crack width limit developed at 445 kN (100 kip).

The maximum deflection for test 1 occurred beneath the load plate on the mid-span side. The deflection of the load plate at the 67 kN (15 kip) load yielded a deflection of 1.14 mm (0.045 in). The 67 kN (15 kip) load was less than the service live load of (16 kip); however, the deflection at 71 kN (16 kip) was calculated by interpolation with the 89 kN (20 kip) increment and was determined to be less than the L/800 AASHTO limit. Figure 3.12 shows the deflection of the load plate for the 67 kN (15 kip) load increment as well as the AASHTO limit and baseline.

The shear failure occurred 712 kN (160 kip), which was 309% of the calculated shear capacity of 230 kN (51.7 kip) (LRFD 5.8.3.3).

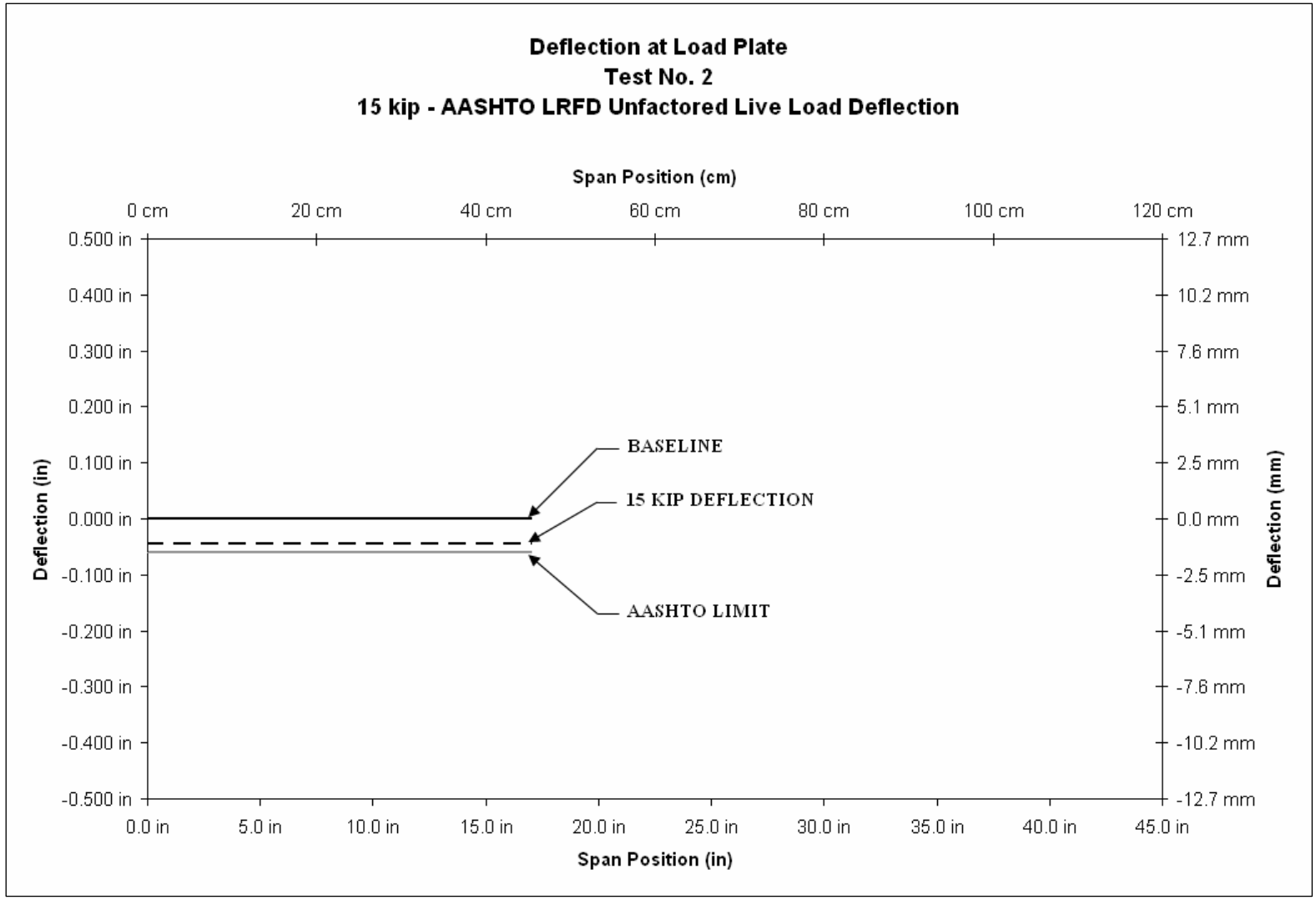

Figure 3.13: Deflection at Load Plate AASHTO Deflection Limit

3.4 Load Test Number Three: S-SB-444-NB-6½

3.4.1 Test Overview

Load test number three differed slightly from tests one and two, in that the center of the load plate was moved to 165 mm (6½ in) from the inside edge of the adjacent haunch. This location was expected to yield higher shear stresses based on early output from the parallel analytical model. The 165 mm (6½ in) value was equal to "d", the distance from the top compressive fiber to the center of gravity of the positive moment reinforcement. The "d" distance from a support is typically used in concrete design as the critical shear section. The new load location was achieved by removing the hydraulic jack and 610 x 749 x 51 mm (24 x 29.5 x 2 in) soffit mounted plate, drilling new holes through the flanges of the transfer girders, and re-attaching the plate and jack in the new location. No bedding material was used during test 1. Prior to the test, the Compumotor indexer/driver malfunctioned and was useless for testing. Consequently, the laser system was unable traverse along the top slab. Readings from the laser deflection system were still recorded; however, the laser was stationary and positioned approximately 25 mm (1 in) from the mid-span edge of the load plate. None of the five applied strain gages survived the casting process. All other systems were fully functional during the test. The concrete compressive strength for this culvert was 8,400 psi.

3.4.2 Crack Propagation

The first hairline crack occurred at 107 kN (24 kip) near the spigot end on the top of the bottom slab, and propagated further until a 156 kN (35 kip) load was reached.

At that load increment, a hairline flexure crack occurred on the bottom of the top slab. Hairline fractures continued to appear and propagate until 289 kN (65 kip). Flexure cracks on the outside of the sidewall closest to the load developed at 311 kN (70 kip) and on the outside of the opposite sidewall at 334 kN (75 kip). Additionally, the first shear crack developed on both the spigot and bell ends at the tip of the haunch adjacent to the load plate around 334 kN (75 kip). A second shear crack on the mid-span side of the load plate appeared at 512 kN (115 kip). Both flexure and shear cracks continued to propagate until ultimate failure occurred at 645 kN (145 kip). The ultimate failure occurred in shear between the load plate and the haunch on the mid-span side. Figure 2.13 provides pictures of each face of the culvert after failure.

Figure 3.14: Test Three Failure

Figure 3.15: Test Three Failure

3.4.3 Deflection Curves

The malfunction of the Compumotor indexer/driver seemed to be a problem; however, after reviewing the inconsistency of the data taken from load test 1, it turned out to be a fortunate loss. The deflection of the top slab was taken at each load increment as in the two prior tests; however, the accuracy of the deflection measurement was greatly increased from the other tests because each recording interval repeated the same measurement. Consequently, any spikes in the data could be easily identified and omitted. The resulting deflection plot is provided in Figure 3.14. The measured deflection points in Figure 3.14 have been extruded to zero for clarity. Additionally, a load vs. deflection curve for the load plate is provided in Figure 3.15.

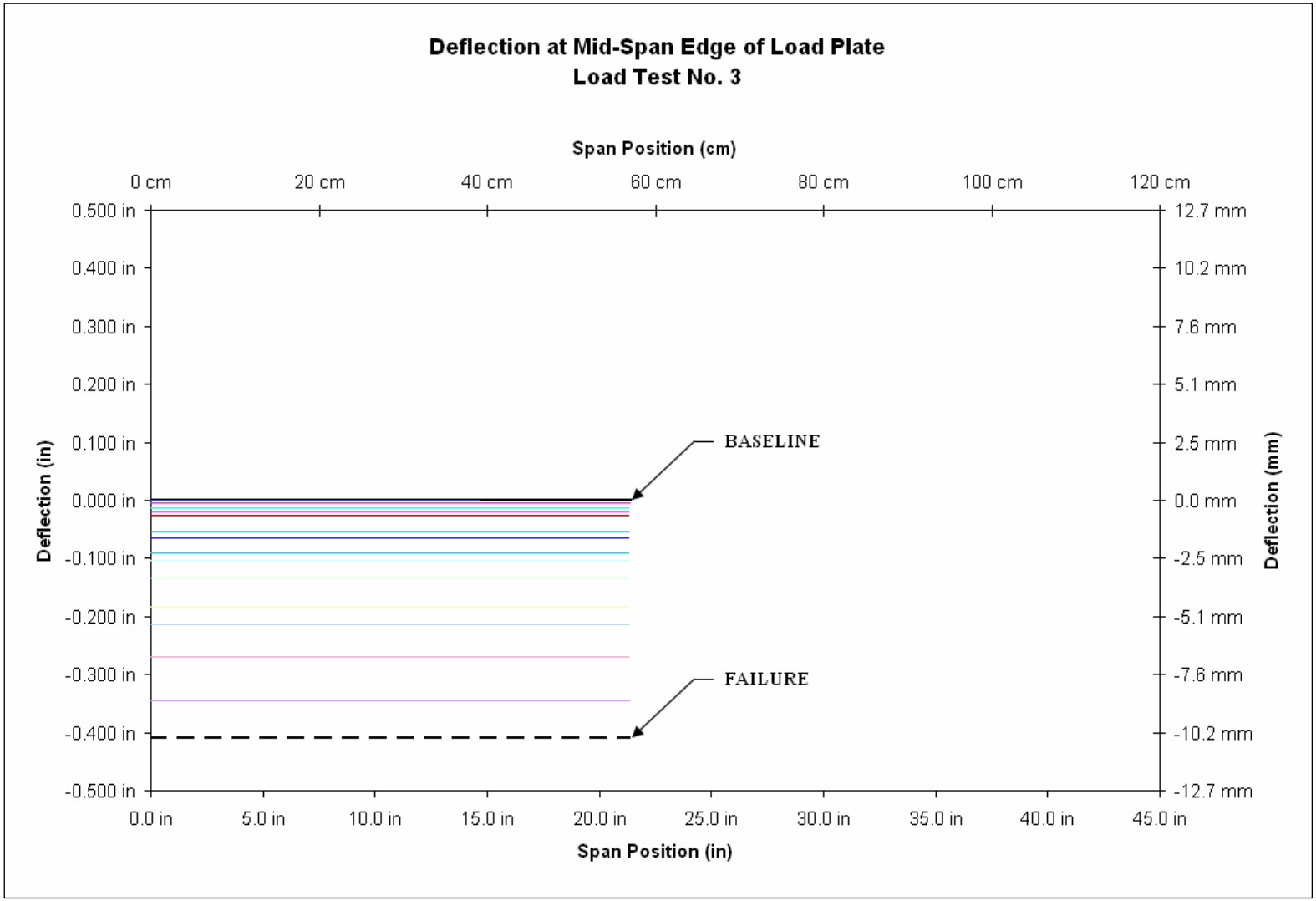

Figure 3.16: Deflection at Load Plate

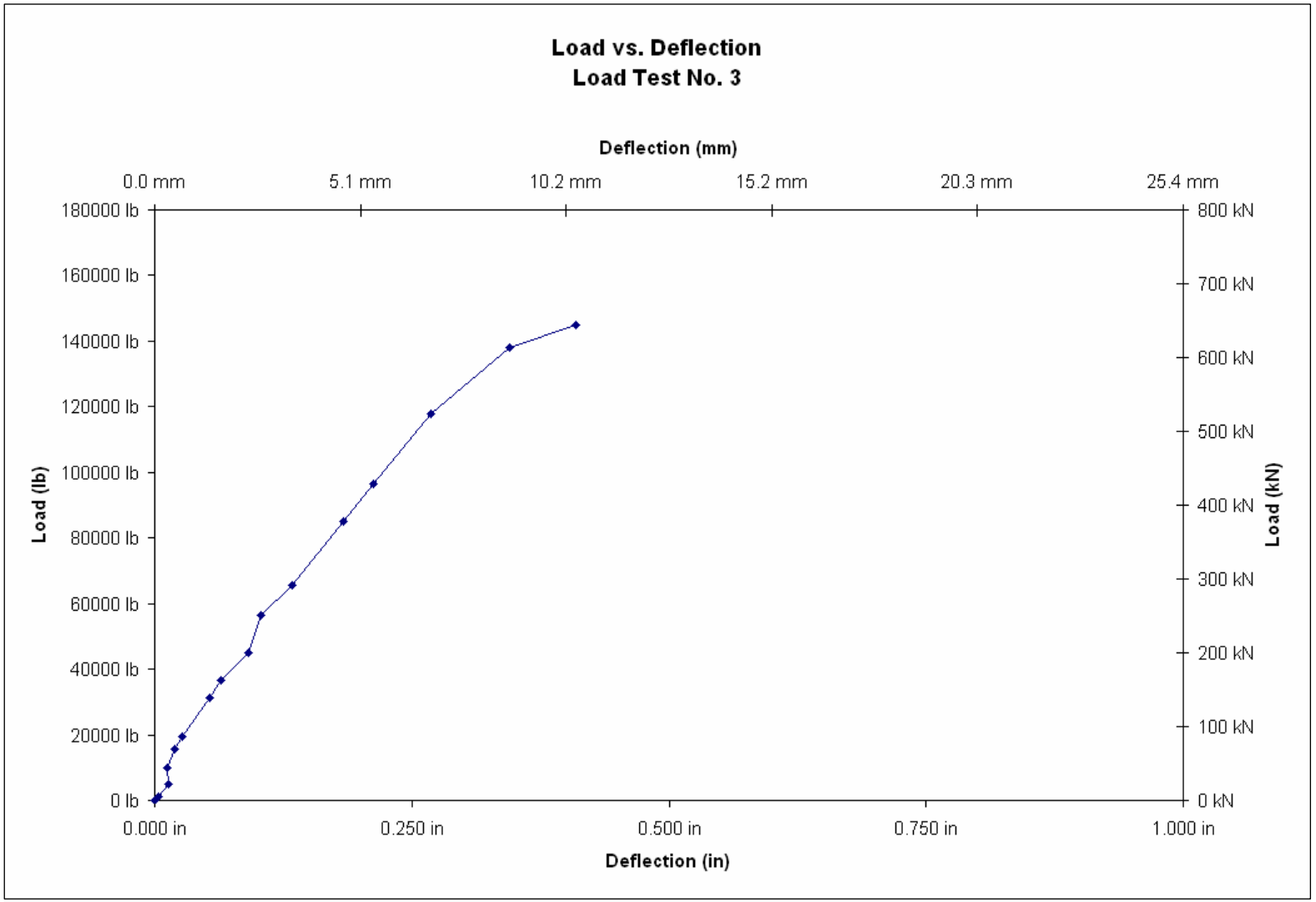

Figure 3.17: Load vs. Deflection

3.4.4 AASHTO Comparisons

The first cracks identified as serviceability failure cracks, those exceeding the 0.33 mm (0.013 in) crack width limit, occurred in flexure at approximately 289 kN (65 kip). The first shear crack to exceed the limit developed at 512 kN (115 kip).

A deflection plot is provided in Figure 3.15 for a service load of 70.3 kN (15.8 kip), which is 0.9 kN (0.2 kip) less than the service limit state load of 71.2 kN (16 kip). The deflection at this load increment was measured to be 0.51 mm (0.02 in), which is less than the AASHTO limit of 1.52 mm (0.06 in) (see Figure 3.16).

The shear failure occurred at 645 kN (145 kip), which is 282% of the calculated shear capacity of 229 kN (51.4 kip) (LRFD 5.8.3.3).

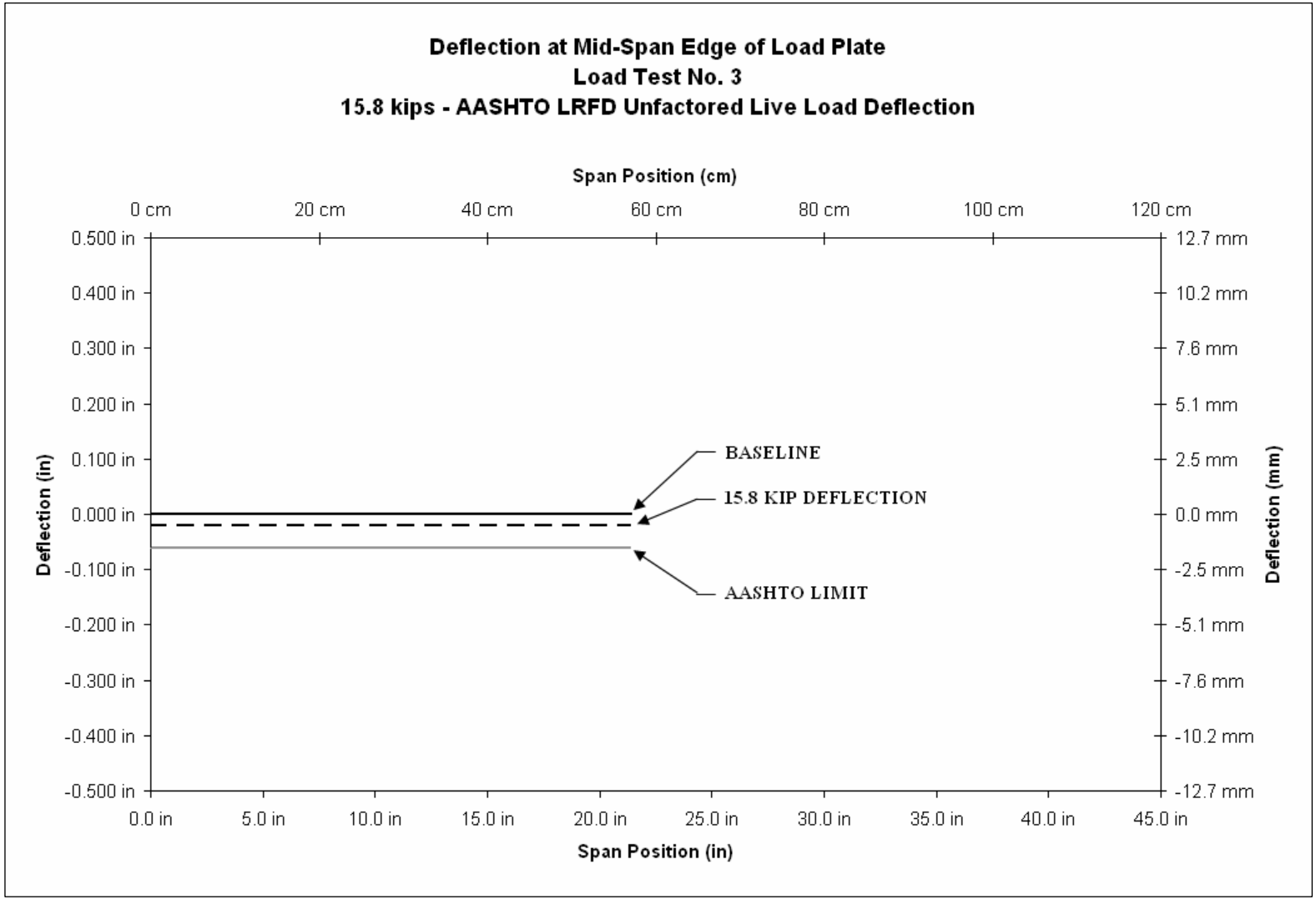

Figure 3.18: Deflection at Load Plate AASHTO Deflection Limit

3.5 Load Test Number Four: S-SB-444-NB-11½

3.5.1 Test Overview

The final load test was performed with the center load plate located 292 mm (11½ in) from the tip of the haunch adjacent to the load plate. This location was determined by the analytical model to yield higher shear stresses in the top slab. The loading system was re-positioned by removing the hydraulic jack and soffit mounted plate, drilling holes in the flanges of the transfer girders, and replacing the jack and plate in their new location. The Compumotor indexer/driver was replaced prior to load test 4, so the laser sensor was allowed to traverse during the test. Three of the five applied strain gages survived the casting process; however, the data obtained was inconclusive and have been omitted from the results. Recommendations regarding strain gages are provided in chapter four. All other instrumentation systems were fully functional during test 4. The compressive strength of the concrete for this culvert was 7,900 psi, which was higher than the design compressive strength of 5,000 psi.

3.5.2 Crack Propagation

Hairline flexure cracks formed at 111 kN (25 kip) and were initiated simultaneously on the top of the bottom slab and the bottom of the top slab. Both cracks extended toward the bell end of the culvert at 133 kN (30 kip). Flexure cracks developed at the bell end (opposite end from the load) near mid-span at 200 kN (45 kip) and continued to propagate as the load increased. Hairline cracks spanning the entire joint length began to develop on the outside of the sidewall adjacent to the load at 245

kN (55 kip). The opposite sidewall experienced similar cracking at 289 kN (65 kip). Also at 289 kN (65 kip), the first serviceability failure crack developed on the bottom of the top slab in flexure. The first hairline shear crack developed between the load plate and adjacent haunch at 400 kN (90 kip). The first shear crack with a width of 0.33 mm (0.013 in) developed between the corner of the load plate and the tip of the haunch opposite of the load at 534 kN (120 kip). Formation and propagation of cracks continued until ultimate failure at 578 kN (130 kip). Failure occurred in shear/bond along the shear crack between the load plate and the opposite haunch. Figure 3.16 provides pictures of each face of the culvert at failure. Failure was believed to be caused by arching where a compressive strut that formed along the shear crack at mid-span buckled and detached from the reinforcement mesh.

Figure 3.19: Test Four Failure

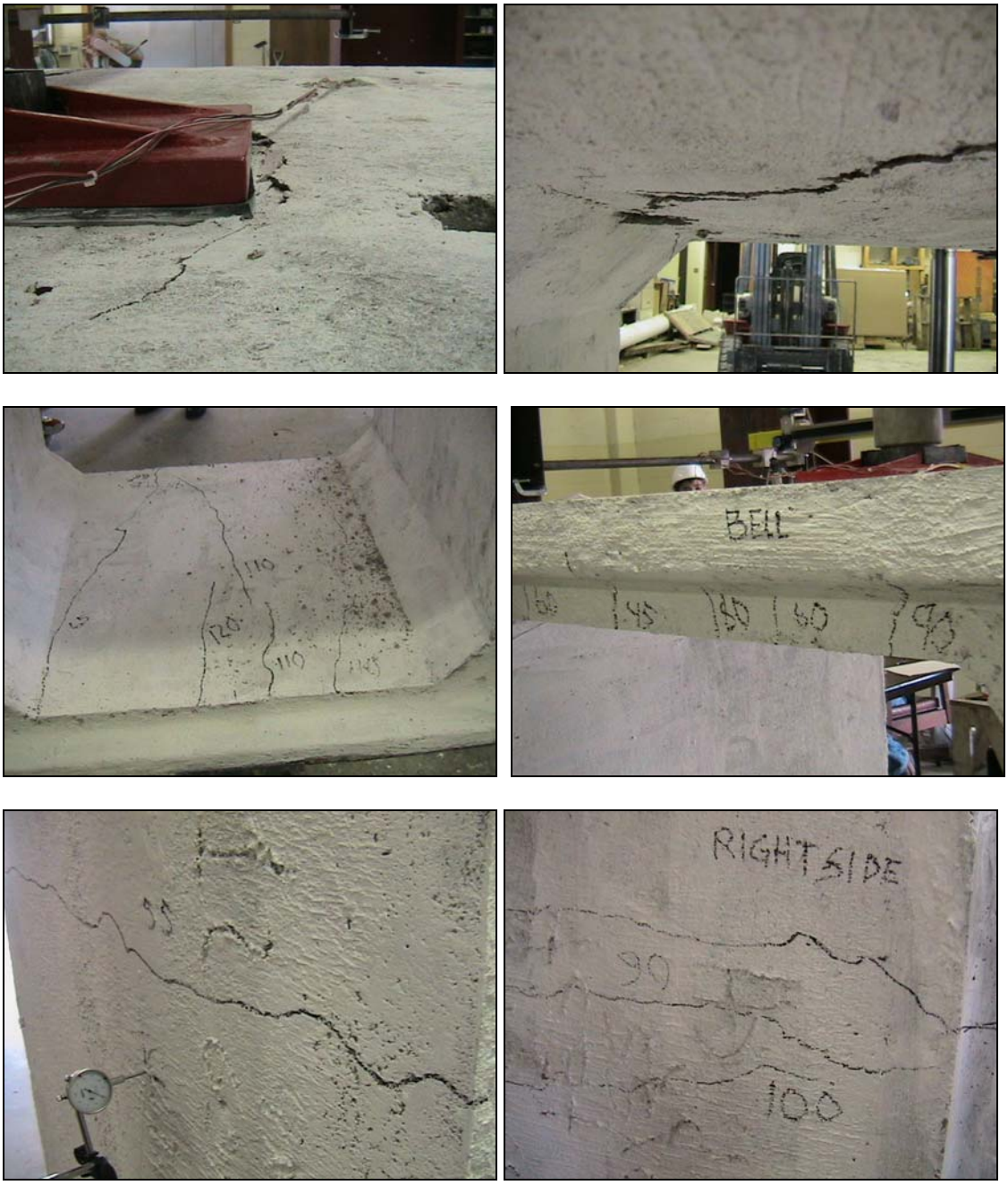

Figure 3.20: Test Four Failure

3.5.3 Deflection Curves

The fourth test utilized the traversing laser deflection system for its measurements. The data for test 1 had not been analyzed prior to test 4; therefore, metallic tape was again used beneath the laser sensor. The tape was not applied to the top of the load plate, so the data there was smooth and useful. The maximum deflection was taken at the mid-span edge of the load plate. Figure 3.18 provides a deflection plot for the load plate at various load increments up to failure. In addition, a load vs. deflection plot is provided as reference for the parallel analytical model (see Figure 3.19). The deflection for test 4 was substantially higher than prior tests, which was expected due to the location of the load plate near mid-span.

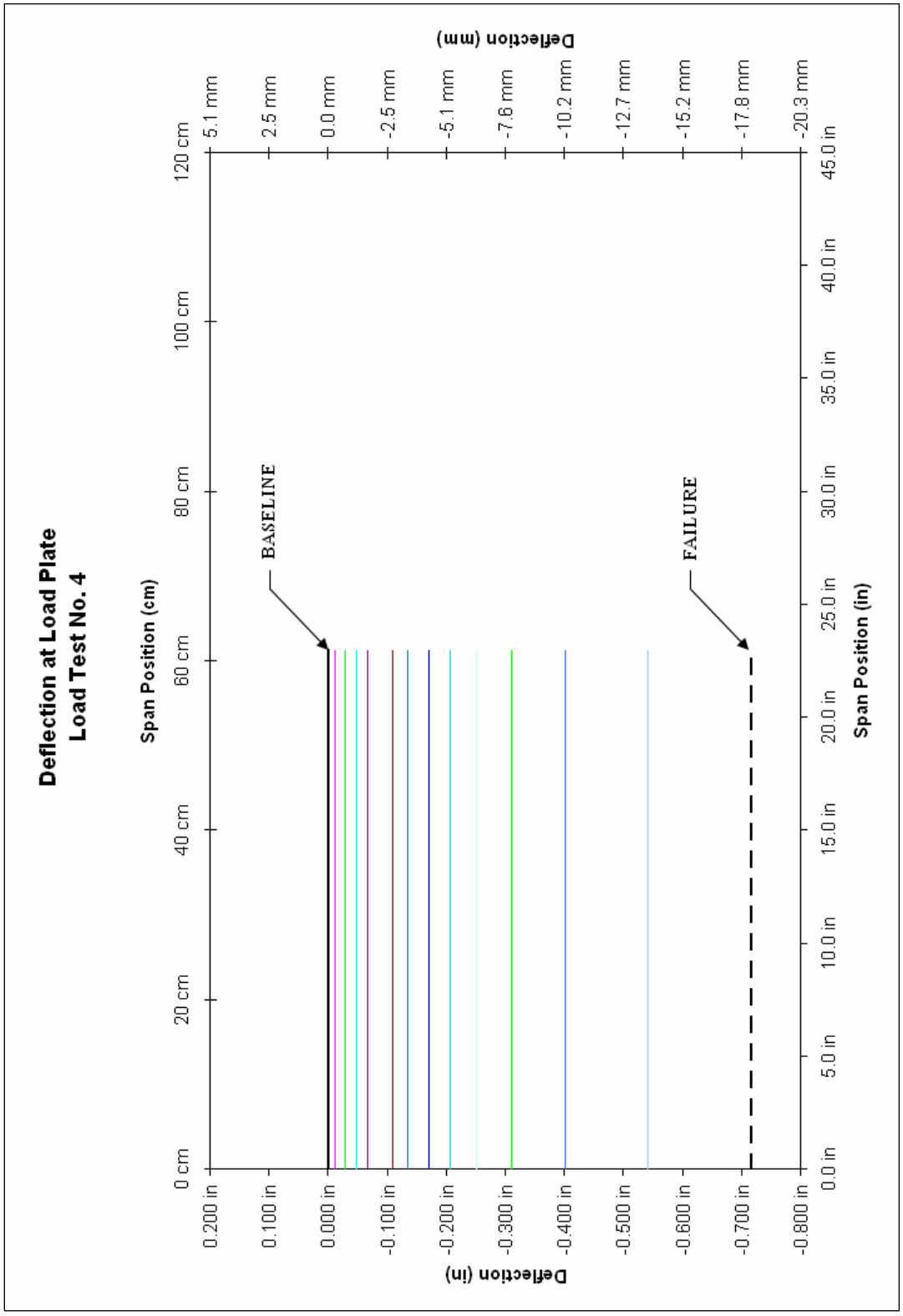

Figure 3.21: Deflection at Load Plate

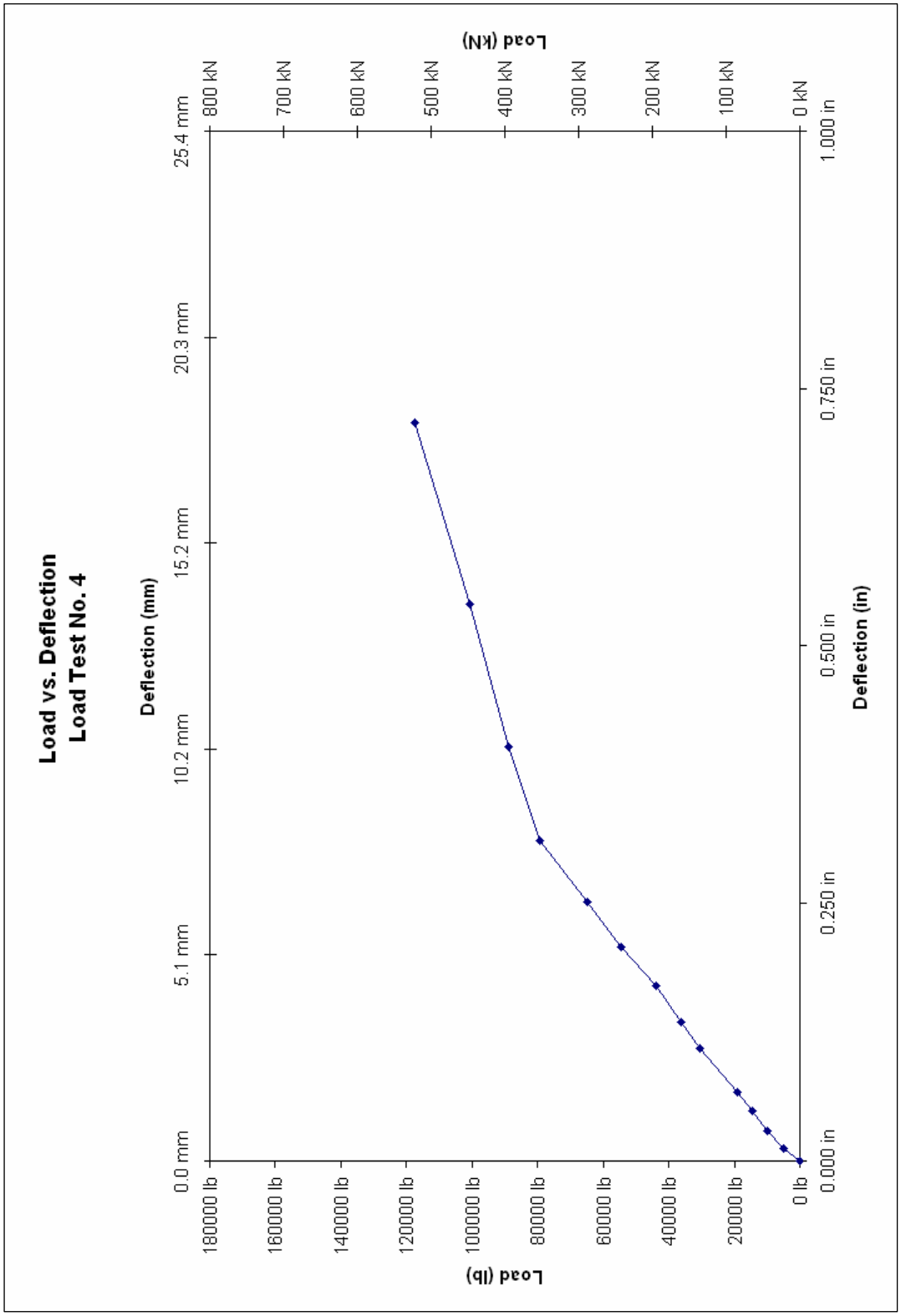

Figure 3.22: Load vs. Deflection

3.5.4 AASHTO Comparisons

The first cracks to exceed the 0.33 mm (0.013 in) limit occurred in flexure at 289 kN (65 kip). The first shear crack to exceed the width limit occurred at 423 kN (95 kip).

The point of maximum deflection was determined at the mid-span edge of the load plate. The deflection at the 67 kN (15 kip) load increment was conservatively determined to be 1.24 mm (0.049 in) which was close to the deflection limit of 1.52 mm (0.06 in) as set by AASHTO LRFD Specifications. The deflection at the 71 kN (16 kip) service load was not recorded, so the value was calculated to be 1.40 mm (0.055 in) by interpolation between the 67 kN and 89 kN (15 kip and 20 kip) measurements. The measurement is very close to the 1.52 mm (0.06 in) limit; however, this was expected since the load was place close to the center of the culvert. Figure 3.20 provides the deflection profile for the 67 kN (15 kip) load increment along with the AASHTO limit and baseline.

The shear failure occurred at 579 kN (130 kip), which is more than double the calculated capacity of 222 kN (49.9 kip) (LRFD 5.8.3.3).

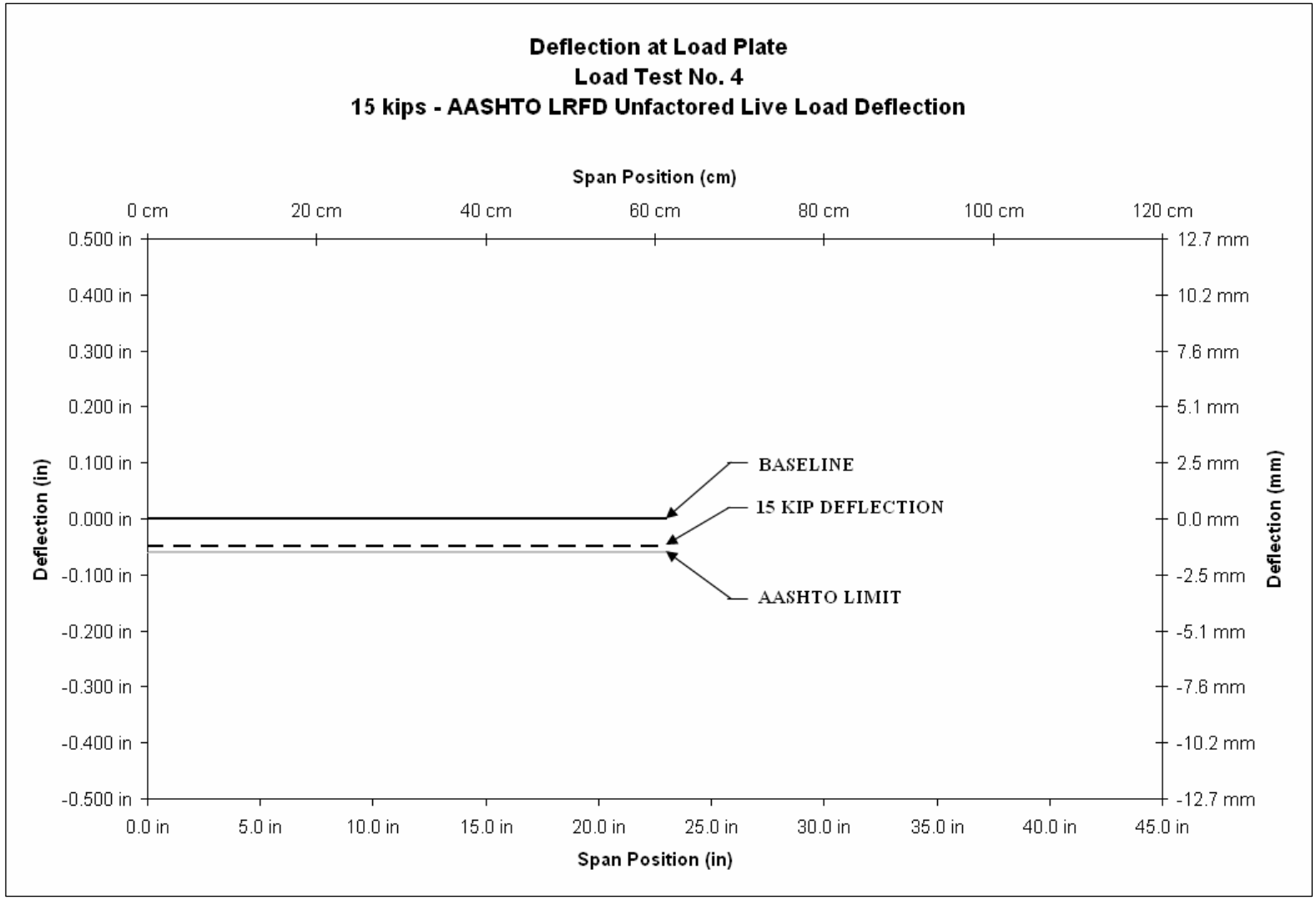

Figure 3.23: Deflection at Load Plate AASHTO Deflection Limit

3.6 Load Test Comparisons

At the conclusion of the four culvert load tests, the results were compared with each other. All culvert tests are directly comparable since the load plate was applied toward on the spigot end. In a broad view, each test culvert behaved in a similar fashion, although each failure load differed. Cracks developed in the same order for each test; beginning with flexural cracks near the spigot end on the top of the bottom slab and the bottom of the top slab. Each culvert experienced cracking of the sidewalls in the range of 267 kN to 400 kN (60 kip to 90 kip). A combined load vs. deflection plot is provided in Figure 3.21 for comparison purposes.

Tests one and two were directly compared for the effects of bedding. They were comparable because the load plate was placed in the same span location, making the use of bedding material the only variable. The initial cracks for tests one and two occurred at 156 kN and 133 kN (35 kip and 30 kip), respectively. The sidewall flexure cracks occurred at 400 kN (90 kip) for test 1 and at 267 kN (60 kip) in test 1. Shear cracks for tests one and two developed at 356 kN and 267 kN (80 kip and 60 kip), respectively. It is likely that the different support conditions lead to the delay in crack development during test 1. Test 1 experienced a gradual flexural failure followed by an abrupt shear failure at 534 kN (120 kip) while test 1 experienced an abrupt shear failure at 712 kN (160 kip).

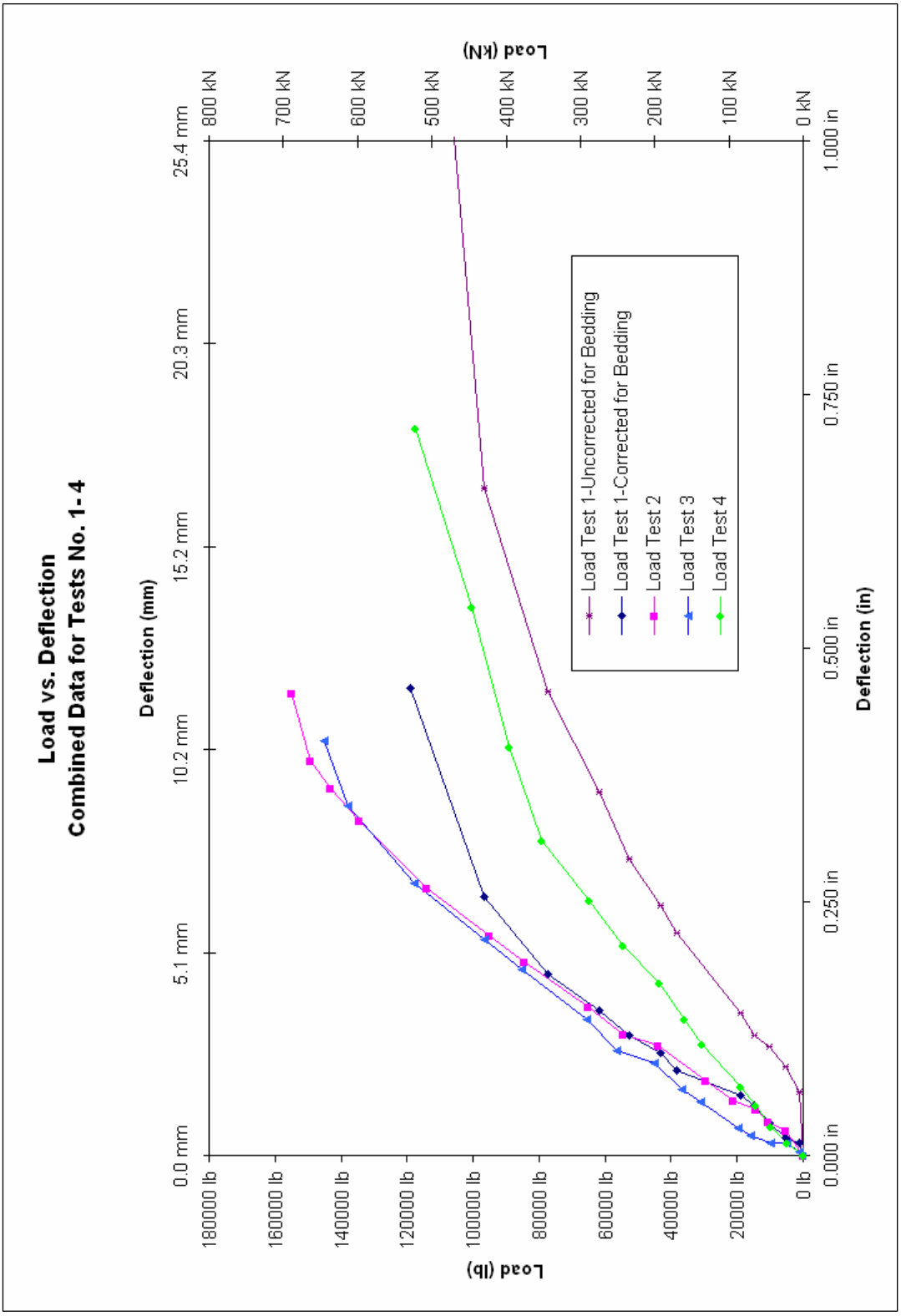

Figure 3.24: Load vs. Deflection Combined Data

Tests two, three, and four were directly compared for shear strength. Due to the consistency in the support condition, the only variable in the test setup was the location of the load relative to the span. The first sign of hairline flexural cracks occurred in the range of 111 kN to 133 kN (25 kip to 30 kip) for each test. The locations of the first cracks were on the bottom of top slab and top of bottom slab on each culvert. The first serviceability failure cracks, those exceeding 0.33 mm (0.013 in) width, developed in flexure over a range of 222 kN to 356 kN (50 kip to 80 kip). Each serviceability failure in flexure was followed by a shear crack exceeding the crack width limit in the range of 423 kN to 512 kN (95 kip to 115 kip).

The load vs. deflection comparison plot in Figure 3.20 is reflective of the anticipated behavior of each culvert. Cracks in test 1 occurred at higher load levels than similar cracks in the other tests. This has been attributed to the bedding material, which provided relief from concentrated stresses and aided in the distribution of loads to the sidewalls and bottom slab. Tests 2 and 3 exhibited very similar behavior, which was expected due to the small difference in the load location [38 mm (1½ in) difference]. Test 4 exhibited higher deflections that were anticipated, since the difference in the load location was substantial [165 mm (6½ in) difference from tests one and two]. Arching is a failure mode between shear and flexure, which differed from the flexure failure that was anticipated. However, it was the goal of the test to isolate shear stresses, and this form of failure accomplished that goal.

CHAPTER IV

SUMMARY, CONCLUSIONS AND RECOMMEDATIONS

4.1 Summary

Load tests were performed on four precast reinforced concrete box culverts for the purposes of shear investigation with regards to AASHTO LRFD Bridge Design Specifications (LRFD 2004, 2005, & 2006). The test culverts measured 1.22 m x 1.22 m x 1.22 m (4 ft x 4 ft x 4 ft) for rise, span, and joint length, respectively and were loaded with a monotonically increasing load through a 254 mm x 508 mm (10 in x 20 in) loading plate. The load plate was located on the free spigot end at a variable distance from the tip of the adjacent haunch: 140 mm (5½ in) for load tests 1 and 2, 165 mm (6½ in) for load test 3, and 292 mm (11½ in) for load test 4. Load test 1 was performed with 76 mm (3 in) of 19 mm (¾ in) graded crushed stone aggregate, while the other test culverts bore directly on the concrete testing floor. Data was collected from each culvert using strain gages, high-resolution laser deflection sensor, load cell, data acquisition hardware and software, and a laptop computer. Tests were monitored for crack propagation, instrumentation input described above, and failure mode.

Cracks occurred in a similar fashion on all test culverts. Each experienced first cracks in flexure on the top of the bottom slab and the bottom of the top slab between a range of 111 kN to 133 kN (25 kip to 30 kip). Serviceability failures occurred first in flexure between the range of 222 kN to 356 kN (50 kip to 80 kip). Shear cracks first

developed within the range of 267 kN to 400 kN (60 kip to 90 kip), with serviceability failure occurring between 423 kN and 512 kN (95 kip and 115 kip). Ultimate failure occurred between 534 kN and 712 kN (120 kip and 160 kip).

4.2 Conclusions

Each culvert tested exhibited behavior that was anticipated. In each case, serviceability requirements for crack width governed failure as opposed to strength requirements. The lowest load at which shear cracks initiated was 267 kN (60 kip) during load test 1. The design load based on current LRFD Specifications is 199 kN (44.7 kip) (LRFD 2006). Comparisons of these loads indicates that 1.22 m x 1.22 m 1.22 m (4 ft x 4 ft x 4 ft) precast reinforced concrete box culverts are adequate in shear, when loaded at a free end. These findings are contradictory to the study by McGrath et al. (2004), which indicated the need for shear transfer at culvert joints and a reduction in shear distribution width for culverts loaded at a free end. Those recommendations eventually lead to the requirement for edge beams that are currently found in the LRFD Specifications (LRFD 2006).

A specific characteristic unique to box culverts was observed during each test, rotation of the corner joints. This phenomenon caused the top slab to undergo additional bending moment at service and factored load; therefore, even though the load plate was placed at approximately the distance equal to the effective depth of the top slab, shear did not govern the behavior. This characteristic behavior was not detected by McGrath et al. (2004).

Table 4.1: Test Summary

Test Identification	First Crack Load		Failure Load	Failure Mode
	Shear	Flexure		
S-SB-444-WB-5	356 kN (80 kip)	156 kN (35 kip)	534 kN (120 kip)	Flexure/Shear
S-SB-444-NB-5	267 kN (60 kip)	133 kN (30 kip)	712 kN (160 kip)	Shear
S-SB-444-NB-6½	334 kN (75 kip)	107 kN (24 kip)	645 kN (145 kip)	Shear
S-SB-444-NB-11½	400 kN (90 kip)	111 kN (25 kip)	578 kN (130 kip)	Shear/Bond

4.3 Recommendations

4.3.1 Instrumentation

The instrumentation systems proved to be adequate for the goal of the shear investigation. Some system outputs were inconclusive, such as the strain gage data; however, provisions can be made to produce useful data during future tests. Changes in procedures are recommended herein for strain gage application, crack width monitoring, and the laser deflection system.

The strain gage application and protection procedures detailed herein provided 30% reliability that the gage would actually function during the load test. This was less than desirable since the application time and expense for each gage was substantial. The violent casting process was deemed responsible for the strain gage malfunctions. A component of the gage application that contributed to this was the connection of the lead wires to the gages. The lead wires that were connected directly to the copper tabs on each gage were relatively bulky and stiff. This likely caused some of the copper tabs to be twisted off during casting, as was often the case during failed applications. To combat this problem, it is recommended that soldering terminals and smooth electrical

wire be used in future applications to transfer current between the lead wires and the copper tabs (see Figure 4.1). The terminals are applied at the same time as the gage using cellophane tape as described in chapter two. Smooth wire is more ductile than encapsulated, braided wire, which allows it to move without breaking or causing damage to the strain gage tabs.

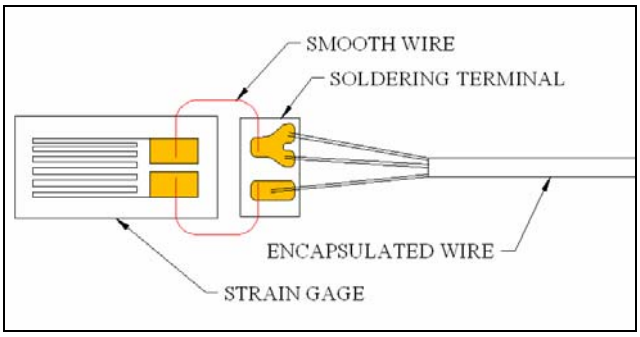

Figure 4.1: Soldering Terminal

Although crack propagation was monitored closely during each test, a feeler gauge was not available for accurate measurement of crack widths. Notes stated "hairline" cracks occurring during each test, which indicate a crack width much less than the 0.33 mm (0.013 in) limit. Each of the 1.22 m x 1.22 m x 1.22 m (4 ft x 4 ft x 4 ft) precast box culverts presented herein likely met the crack control limits of AASHTO LRFD 5.7.3.4; however, it is recommended in future tests that crack widths be precisely monitored using a 0.33 mm (0.013 in) thick feeler gauge.

The laser deflection system provided useful data for all four tests; however, the profile of the each culvert's top slab could have been much smoother. The laser was projected onto the culvert's surface during load test 1 and was projected onto metallic

tape during load tests two and four. Load test 1 provided the highest level of accuracy for the laser deflection profile measurements; however, the data produced could have been better. It is recommended for future tests that a (1 in) wide 0.8 mm (1/32 in) thick strip of balsa wood be glued to the surface using a low-strength adhesive. Balsa wood is inherently strong enough not to transfer the rough contours of the culvert surface, but weak enough as to not add strength to the compression zone of the concrete section. Several other materials are available to achieve the desired result of providing a smooth surface without affecting the strength of the culvert.

4.3.2 Future Load Tests

Load tests were performed on the free spigot end of four 1.22 m x 1.22 m x 1.22 m (4 ft x 4 ft x 4 ft) precast box culverts. The governing LRFD criteria for such culverts include span lengths up to 4.6 m (15 ft) with no limit on joint length or rise (LRFD 2006). It is recommended that future tests be performed on culverts of different span and joint length configurations as presented in Table 4.2 (reference section 3.1 for culvert identification). The culverts listed will provide a wide range of structural behavior data for the parallel analytical model and justification for any recommended changes to future specifications. In addition it is recommended that a variety of manufacturers be used to verify the findings for the entire culvert industry.

Table 4.2: Future Load Test Recommendations

Culvert Identification	No. of Culverts	Notes
S-SB-444-NB-O	2	Use Different Manufacturer From Original Tests
B-SB-444-NB-O	1	
S-DB-444-NB-O	1	Investigate Load Transfer Through Joints
S-SB-844-NB-O	2-3	
B-SB-844-NB-O	1	
S-SB-1244-NB-O	2	12 ft Span Length
S-SB-1246-NB-O	2	12 ft Span Length; 6 ft Joint Length

(See section 3.1 for culvert identification key)

4.3.3 Analytical Model

The scope of the research detailed herein was to investigate the shear capacity of precast reinforced concrete box culverts. Each physical load test performed costs a substantial amount of money both directly, through material costs, and indirectly, through time and instrumentation expenses. The use of analytical analysis provides the benefit of justifiable results with out the accompanying costs. Each physical load test provides a plethora of data that can be utilized for convergence of the analytical model. Once the model achieves convergence, new variables, such as lateral earth pressure, bedding reactions, and material strengths, can be introduced to the model without cost. Consequently, thousands of scenarios can be simulated and the data analyzed with high levels of accuracy. It is recommended that the analytical model provide data analysis for variable culvert sizes and in-service conditions with the ultimate goal of determining new criteria for the design of precast reinforced concrete box culverts. Previous research utilized two-dimensional finite elements for analytical analysis, which generally only accounts for the inherent stiffness of the concrete. It is recommended

that the parallel analytical model utilize three-dimensional elements with the stiffness of the concrete and steel accounted for in the structural properties.

4.3.4 AASHTO LRFD Bridge Design Specifications

The specifications governing the design of precast reinforced concrete box culverts are currently presented jointly with cast-in-place box culverts and arches (LRFD 2006, Section 12.11). Certain criteria for cast-in-place culverts and precast culverts are separate, for instance, the 'Minimum Reinforcement' criteria in Section 12.11.4.3 (LRFD 2006) and concrete cover requirements. However, other criterion is utilized jointly regardless of the casting method; such as 'Loads and Live Load Distribution' which includes a provision for edge beams in Section 12.11.2.1 (LRFD 2005).

The edge beam criterion presented in Section 12.11.2 (LRFD 2005) is based on analytical research (McGrath et al. 2004) for span lengths of 2.44 m (8 ft) or more with a 9.14 m (30 ft) joint length. The analytical model utilized a HS20 axle load [two wheels spaced at 1.83 m (6 ft)] with the outside wheel placed on the free culvert end. The analytical model produced a live distribution width, which eventually lead to an edge beam requirement for box culverts loaded within 0.61 m (2 ft) of the free end. The data, while reliable for a 9.14 m (30 ft) joint length, is not valid for precast culverts with joint lengths less than 2.34 m (7.67 ft) because two wheel loads cannot be applied simultaneously to the top slab. Additionally, the study was not compared with experimental test results, making the findings and recommendations subject to scrutiny. The results of the research detailed herein indicate that joint rotations cause the

governing failure mode to be serviceability cracking, not shear. Therefore, it is recommended that precast box culverts with joint lengths less than 2.34 m (7.67 ft) be exempt from the edge beam criteria in Section 12.11.2.1 (LRFD 2005) pending further investigation.

APPENDIX A

DESIGN EXAMPLE

LRFD DESIGN EXAMPLE:

1.22 m x 1.22 m x1.22m (4 ft x 4 ft x 4 ft) BOX CULVERT TOP SLAB

(US Customary Units)

References

AASHTO LRFD Bridge Design Specifications (LRFD 2004, 2005, 2006)
BOXCAR Box Culvert Design Software

Assumed Values

Clear Span, s:	4.0 ft
Rise, r:	4.0 ft
Joint Length, *l*:	4.0 ft
T^t_{slab}:	7½ in
T^b_{slab}:	6 in
T_{wall}:	5 in
Haunch Size, h:	5 in
Soil Unit Weight, γ_s:	120 lb/ft^3
Concrete Unit Weight, γ_c:	150 lb/ft^3
Outside Concrete Cover, Co:	1 in
Inside Concrete Cover, Ci:	1 in
Top Slab Only, Co^t:	2 in
Height of Fill, H:	1.5 ft

Load Factors		Tables 3.4.1-1 and 3.4.1-2, Strength I
Dead Load, DC:	1.25	
Live Load, LL:	1.75	
Vertical Earth Load, EV:	1.30	
Multiple Presence Factor, mp:	1.20	Article 3.6.1.1.2
Dynamic Load Allowance, IM_f:	26.81%	Article 3.6.2.2

Load Modifiers Section 1.3.2

Ductility, η_D:	1.00	Article 1.3.3
Redundancy, η_R:	1.05	Articles 1.3.4 and 12.5.4
Importance, η_I:	1.00	Articles 1.3.5 and 3.10.3

Strength Reduction Factors Table 12.5.5-1

Flexure, Φ_f:	1.00
Shear, Φ_v:	0.90

Design Calculations

Dead Load

Soil Dead Load

$$W_{soil} = \gamma_s \times H \times l = 120\frac{lb}{ft^3} \times 1.5\,ft \times 4\,ft = 720\frac{lb}{ft} = 0.72\frac{k}{ft}$$

Concrete Dead Load

$$W_{conc} = \gamma_c \times T_{slab}^{t} \times l' = 150\frac{lb}{ft^3} \times \frac{7\,\frac{1}{2}\,in}{12\,\frac{in}{ft}} \times 4.33\,ft = 406\frac{lb}{ft} = 0.41\frac{k}{ft}$$

l' is includes the joint length plus 4" (spigot and bell) for dead load only

Live Load

Live Load Distribution Width, E Article 4.6.2.10.2

Moment and Shear Live Load Distribution

E = 96 + 1.44s = 101.76 in < 48 in => use 48 in

Wheel Load

P_w = 16 kip

Lane Load

Not required per LRFD 3.6.1.3.3 (LRFD 2005)

Structural Analysis Using BOXCAR

Reinforcement Required (See Figure A.1)

A_S1	0.180 in^2/ft	A_S5	0.198 in^2/ft
A_S2	0.397 in^2/ft	A_S6	0.180 in^2/ft
A_S3	0.251 in^2/ft	A_S7	0.180 in^2/ft
A_S4	0.120 in^2/ft	A_S8	0.144 in^2/ft

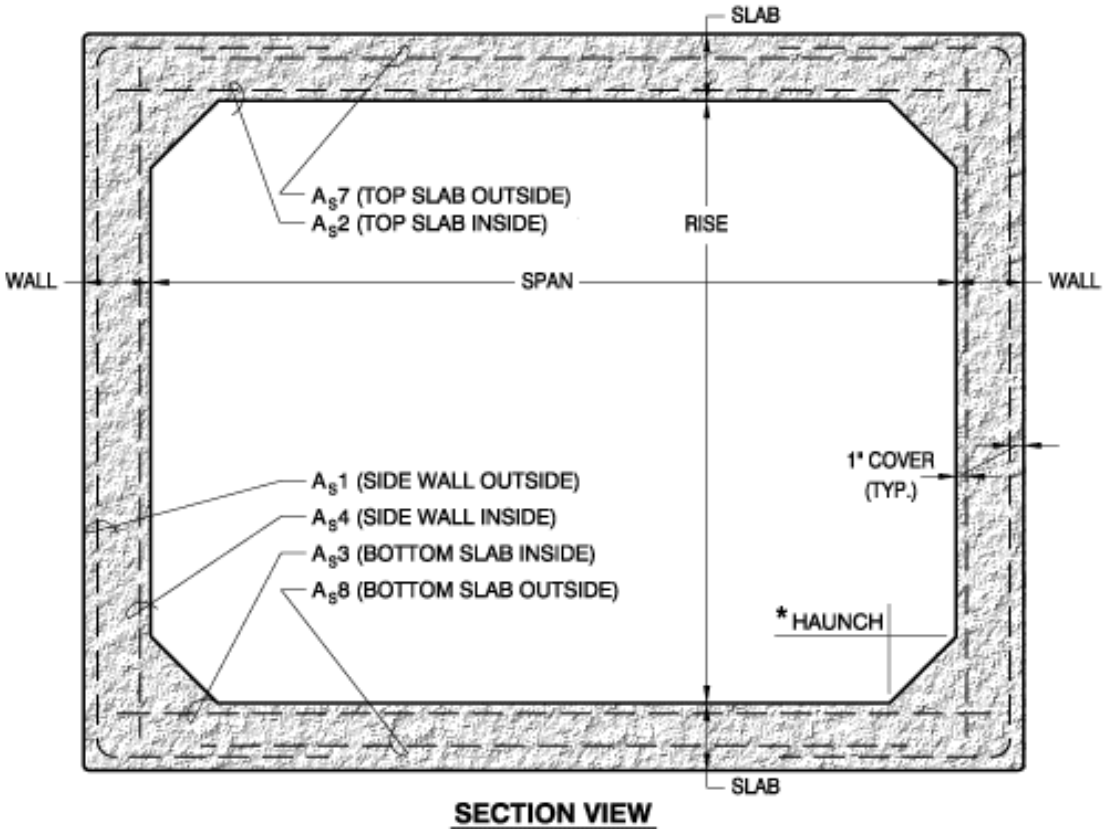

Figure A.1: Culvert Reinforcement

REFERENCES

American Association of State Highway and Transportation Officials (2004), AASHTO LRFD Bridge Design Specifications, 3rd Ed., AASHTO, Washington, D.C.

American Association of State Highway and Transportation Officials (2005), AASHTO LRFD Bridge Design Specifications, 3rd Ed., 2005 Interim Revisions, AASHTO, Washington, D.C.

American Association of State Highway and Transportation Officials (2006), AASHTO LRFD Bridge Design Specifications, 3rd Ed., 2006 Interim Revisions, AASHTO, Washington, D.C.

American Association of State Highway and Transportation Officials (2002), AASHTO Standard Specifications for Highway Bridges, 9th Ed., AASHTO, Washington, D.C.

American Society for Testing and Materials (ASTM) International (2001). "A185-(2001): Standard Specification for Steel Welded Wire Reinforcement, Plain, for Concrete." ASTM International, West Conshohocken, PA.

American Society for Testing and Materials (ASTM) International (2001). "A497-(2001): Standard Specification for Steel Welded Wire Reinforcement, Deformed, for Concrete." ASTM International, West Conshohocken, PA.

American Society for Testing and Materials (ASTM) International (2003). "C1433-03: Standard Specification for Precast Reinforced Concrete Box Sections for Culverts, Storm Drains, and Sewers." ASTM International, West Conshohocken, PA.

American Concrete Institute (2005). "ACI 318-05, Building code requirements for structural concrete and commentary." ACI, Farmington Hills, MI.

American Concrete Pipe Association (2000). Concrete Pipe Design Manual, American Concrete Pipe Association, Irving, Texas.

Glenn Weinreb Inc, (2003). instruNet® Users Manual, version 2.0, GWI, USA

James, Ray W. (1984). "Behavior of ASTM C 850 Concrete Box Culverts Without Shear Connectors." *Transportation Research Record 1001*, Transportation Research Board, National Research council, Washington D.C., pp 104-111.

Federick, G.R., Ardis, C.V., Tarhini, K.M., and Koo, B. (1988). "Investigation of The Structural Adequacy Of C 850 Box Culverts," *Transportation Research Record 1191*, Transportation Research Board, National Research council, Washington D.C., pp 73-80.

Sonnenberg, A. M. C., Al-Mahaidi, R., and Taplin,G. (2003). "Behavior of Concrete Under Shear and Normal Stresses." *Magazine of Concrete Research.* 55 (4) 367-372.

McGrath, Timothy J., Liepins, Atis A., Beaver, Jesse L. and Strohman, Bryan P., (2004). "Live Load Distribution Widths for Reinforced Concrete Box Culverts." A study for the Pennsylvania Department of Transportation, Simpson Gumpertz & Heger Inc, Boston.

Smeltzer, Paul and Bentz, Evans. (2004). "Research Suggests Conservative Design of Concrete Box Culverts." Environmental Science & Engineering Magazine, <http://www.esemag.com>May 2004.

Yee, R.A., Bentz, E.C., Collins, M.P., (2004), "Shear Behavior of Concrete Box Culverts: A Preliminary Study", Department of Civil Engineering, University of Toronto, Toronto, Canada.

BIOGRAPHICAL INFORMATION

Jarrod Clinton Burns was born on December 27, 1982 in New Port News, Virginia, adjacent to Langley Air Force Base where his father was stationed as a member of the United States Air Force. After living in various locations around the world, he settled in Cabot, Arkansas and later graduated from Cabot High School in the year 2000. Jarrod attended the University of Arkansas in Fayetteville from August 2000 until May 2004, when he graduated Summa Cum Laude with a Bachelor of Science in Civil Engineering. He earned his Engineer-In-Training certification from the Arkansas State Board of Registration for Professional Engineers and Land Surveyors by examination in June 2004.

Immediately upon graduation, Jarrod became employed with Lockwood, Andrews & Newnam, Inc. in Houston, Texas. His duties included structural engineering services for the design and evaluation of concrete and steel pressure pipe, concrete buildings, highway bridges, and aerial structures for light-rail and commuter-rail systems across the state of Texas.

Jarrod enrolled in the graduate program for Civil Engineering at the University of Arkansas in fall 2004, and transferred to the comparable program at the University of Texas at Arlington in spring 2005. He was awarded an Eisenhower Transportation Fellowship from the National Highway Institute, which funded his education and research efforts during his two years at UTA. He performed research under the

supervision of Dr. Ali Abolmaali towards the degree of Masters of Science in Civil Engineering with an emphasis on structural engineering. Jarrod plans to continue employment with Lockwood, Andrews & Newnam, Inc. in Houston, Texas and to apply for professional registration in 2007.